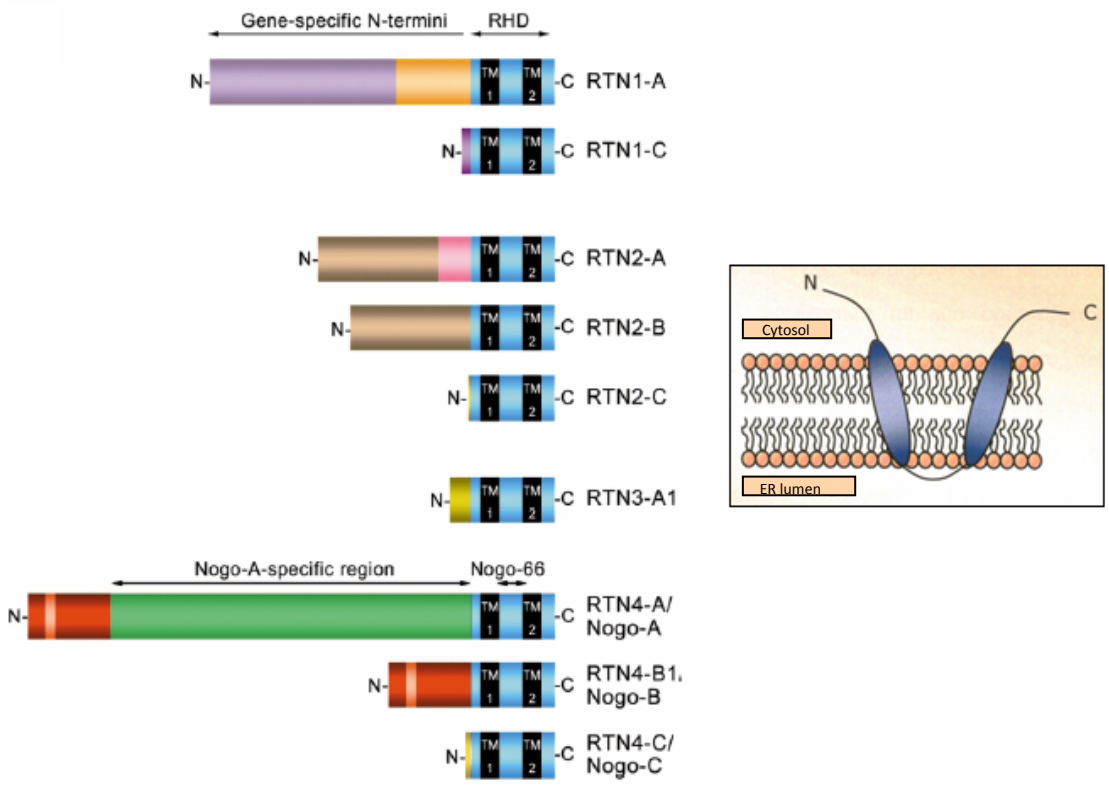

Fig 1.1. The reticulon gene family . (Adapted from Schwab and Oertle, 2003)
A scheme showing the different types of reticulon family members. RTN: reticulon, RHD: rel homology domain,Nogo: neurite outgrowth inhibitor, ER: endoplasmic reticulum.

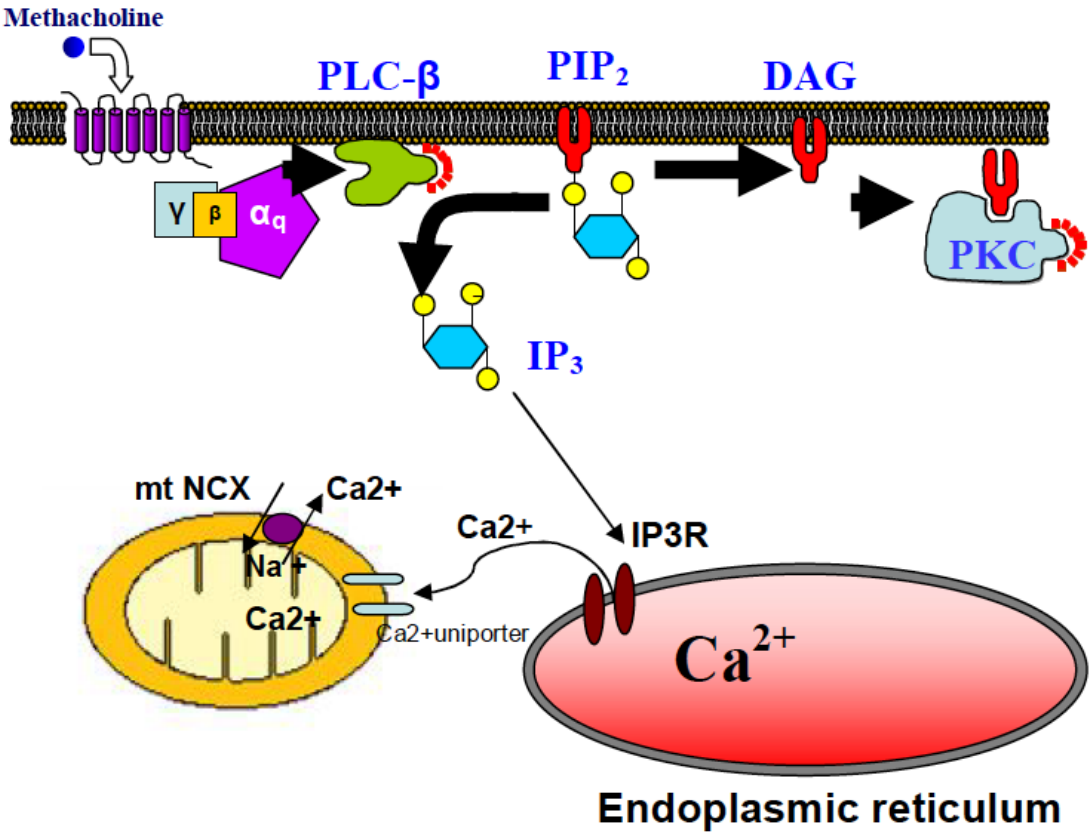

Fig 1.2. A schematic of methacholine activated muscarinic M3-receptor signalling pathway. This figure shows the muscarinic pathway used in some of the experiments conducted in chapter 3 as described in the text.PLC-β: phospholipase C beta, PIP_2: phosphatidyl inositol bisphosphate, DAG: diacylglycerol, PKC: protein kinase C, IP_3: inositol trisphosphate, IP_3R: inositol trisphosphate receptor, mt NCX: mitochondrial sodium calcium exchanger.

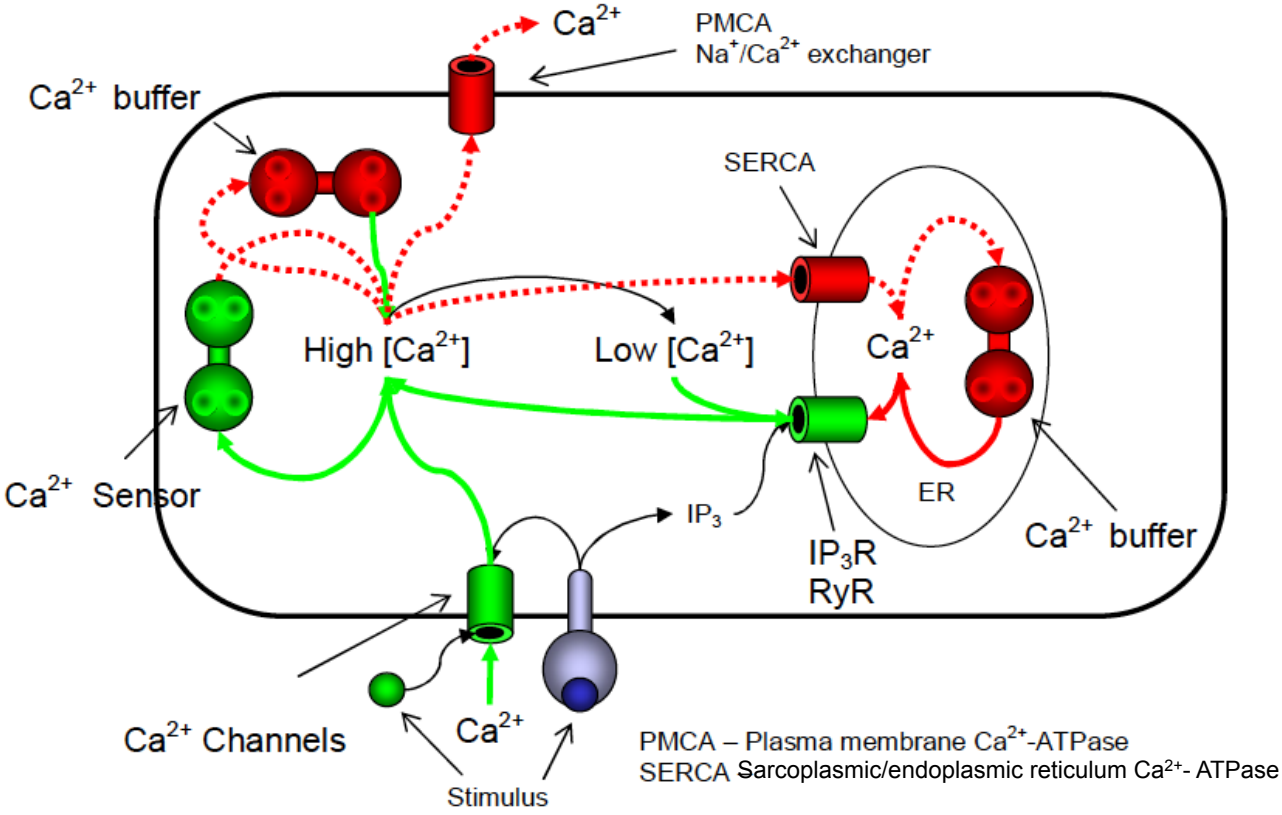

Fig 1.3. A schematic of on/off mechanisms of Ca^{2+} dynamics in living cells. (www.cellsignallingbiology.org). This scheme describes various mechanisms through which Ca^{2+} influx and efflux can occur. (RyR: ryanodine receptor, IP3R: inositol trisphosphate receptor.

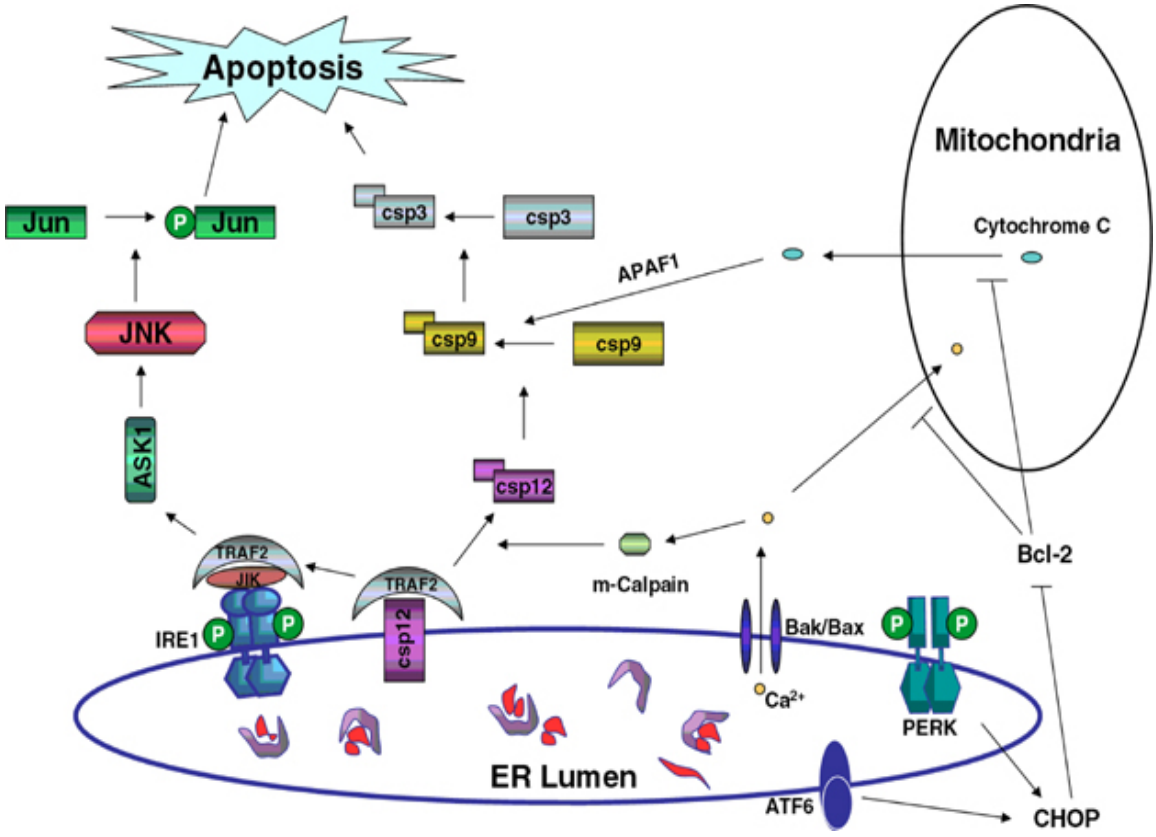

Fig 1.4. A link between ER stress, JNK and apoptosis. (Adapted from Wu and Kaufman, 2006). This figure illustrates the different cellular pathways activated in ER stress.Csp: caspase, Apaf1: apoptotic protease activating factor-1, JNK:c-JUN NH2- terminal kinase , ASK1: signal -regulating kinase 1, TRAF2:TNF receptor−associated factor 2, IRE1: inositol requiring enzyme 1, Bcl-2: B-cell lymphoma 2 , Bak/Bax:Bcl-2 antagonist killer/ Bcl-2 associated x protein , ATF: activating transcription factor, PERK:protein kinase RNA−like endoplasmic reticulum kinase , CHOP:C/EBP homologous protein

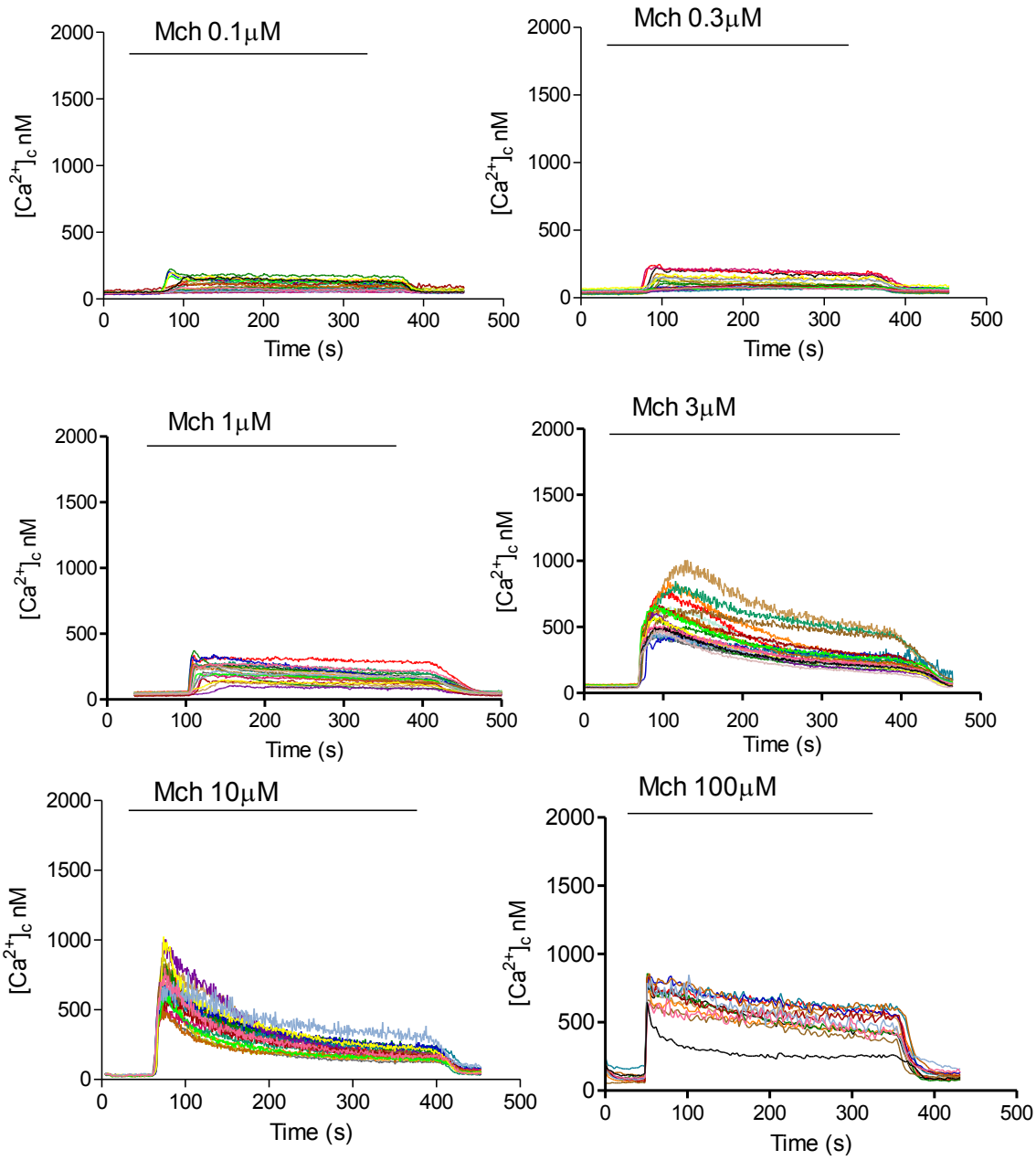

Fig. 3.1. Characterization of muscarinic receptor activation-induced cytosolic Ca^{2+} signals in SH-SY5Y cells.

Cells loaded with fura-2 (2μM 1h), mounted on an epifluorescent microscope, were perfused with KHB for the first 30s and then were perfused with Mch at a range of concentrations (0.1, 0.3, 1, 10, 100μM) for 5 min before washing the drug for 2min. Data are representative of 41 to 77 cells from 2 to 3 experiments for each condition.

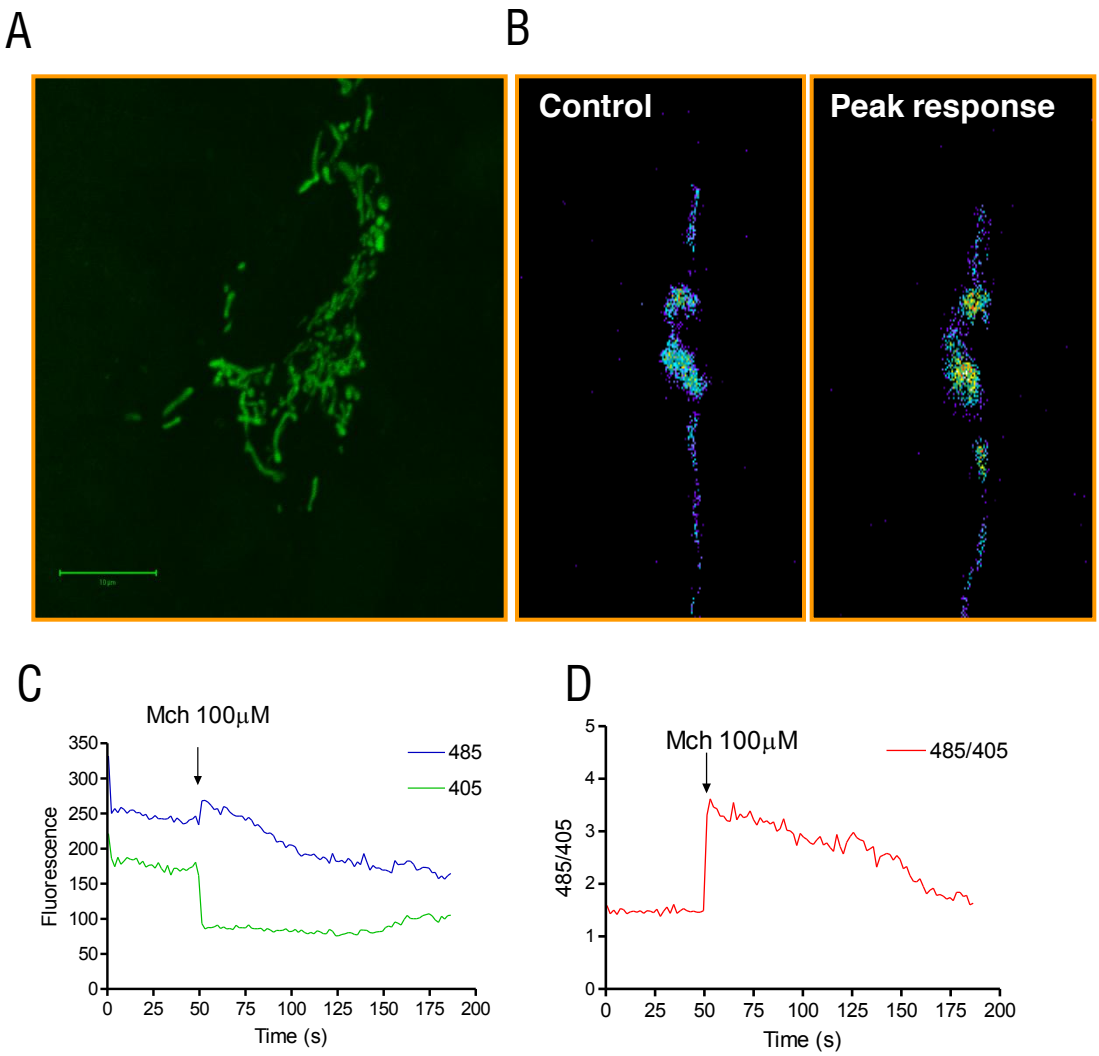

Fig. 3.2. Measuring mitochondrial Ca^{2+} signals in SH-SY5Y cells.

(A) A transfected cell with plasmid expressing 2mtRP imaged by confocal microscopy by using a x63 objective (plus x4 optical zoom), with an optical depth of 1µm. (B) Representation of mitochondrial Ca^{2+} changes generated by muscarinic receptor activation taken by epifluorescent microscopy. Pseudocolor representation of changes in mtiochondrial Ca^{2+} levels in a SH-SY5Y cell transfected with plasmid expressing 2mtRP. Images are shown before stimulation, and at mitochondrial maximal response. Mitochondrial Ca^{2+} increases are indicated by pseudocolor changes from blue / green to yellow/ red. (C) An example of pericam emissions in SH-SY5Y cells after stimulation with Mch 100µM for 1min, followed by 90 s wash out with KHB. Pericam is excited by 485 nm and 405 nm wave-lengths. (D) The ratio (485/405) indicates mitochondrial Ca^{2+} levels in the cell shown in (C). When emission signal of the 485/405 ratio rises, this indicates an increase in mitochondrial Ca^{2+} levels.

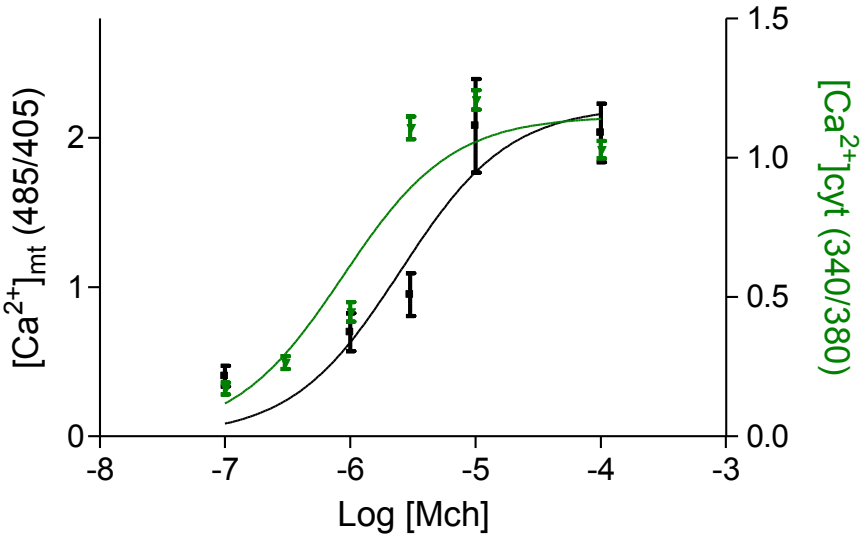

Fig. 3.3. Concentration-response curves for cytosolic and mitochondrial Ca^{2+} responses.

Two concentration-response curves were constructed using the peak-basal value from both cytosolic and mitochondrial Ca^{2+} peak responses. The EC_{50} values for Mch in cytoslic and mitochondrial Ca^{2+} were 0.8 and 3.45μM, respectively.

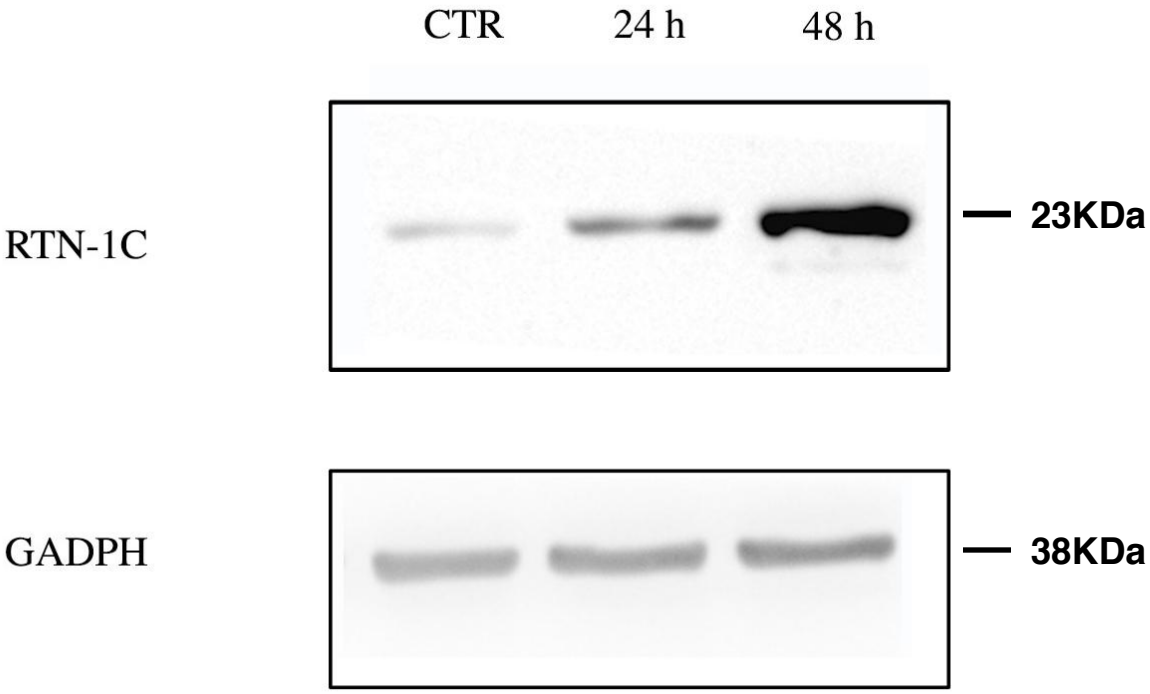

Fig. 3.4. RTN-1C expression level.
SH-SY5Y neuroblastoma cells were transiently transfected with an expression construct carrying the cDNA for RTN1-C (Fazi et al, 2009) or the vector alone (CTR) for 24 and 48 hours. Cells were then lysed, harvested and western blot analysis was performed. Membranes were probed with an anti-RTN1C (1:1000) and GAPDH (1:25000). The results shown are representative of three independent experiments.

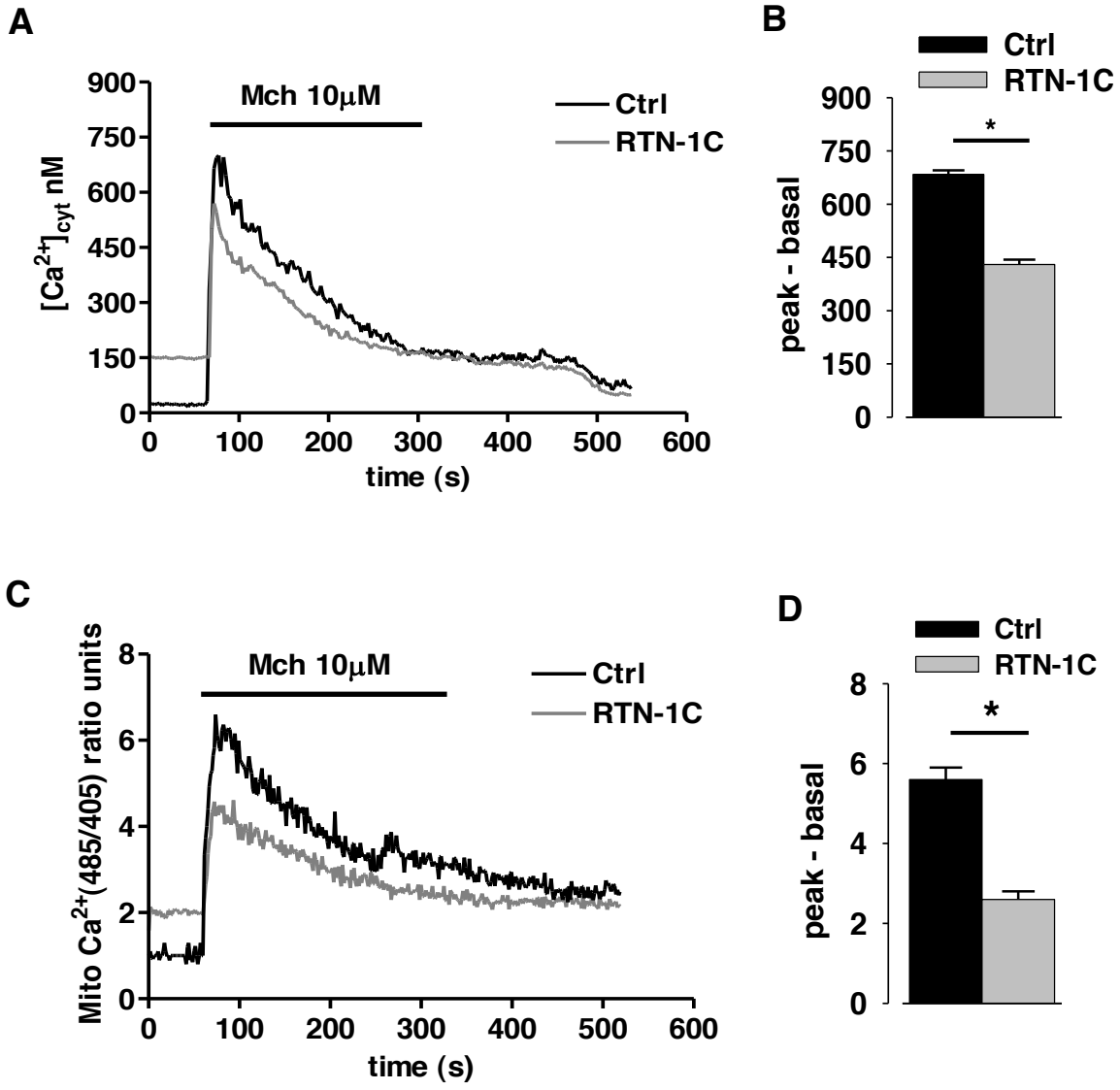

Fig. 3.5. Methacholine induced cytosolic and mitochondrial Ca^{2+} signals in RTN1C overexpressing SH-SY5Y cells. (A) Control and RTN1C overexpressing cells were loaded with fura-2(2μM 1h), and perfused with Mch (10 μM).(B) Quantification of cytosolic basal and peak-basal values of Ca^{2+} responses to Mch 10μM. (C) Cells transfected with 2mtRP were perfused with Mch (10 μM). (D) Quantification of mitochondrial Ca^{2+} responses to Mch 10μM.Unpaired Student's *t*-test, $P<0.05$ for each condition *vs* control. Data are representative of 3 experiments for each condition.

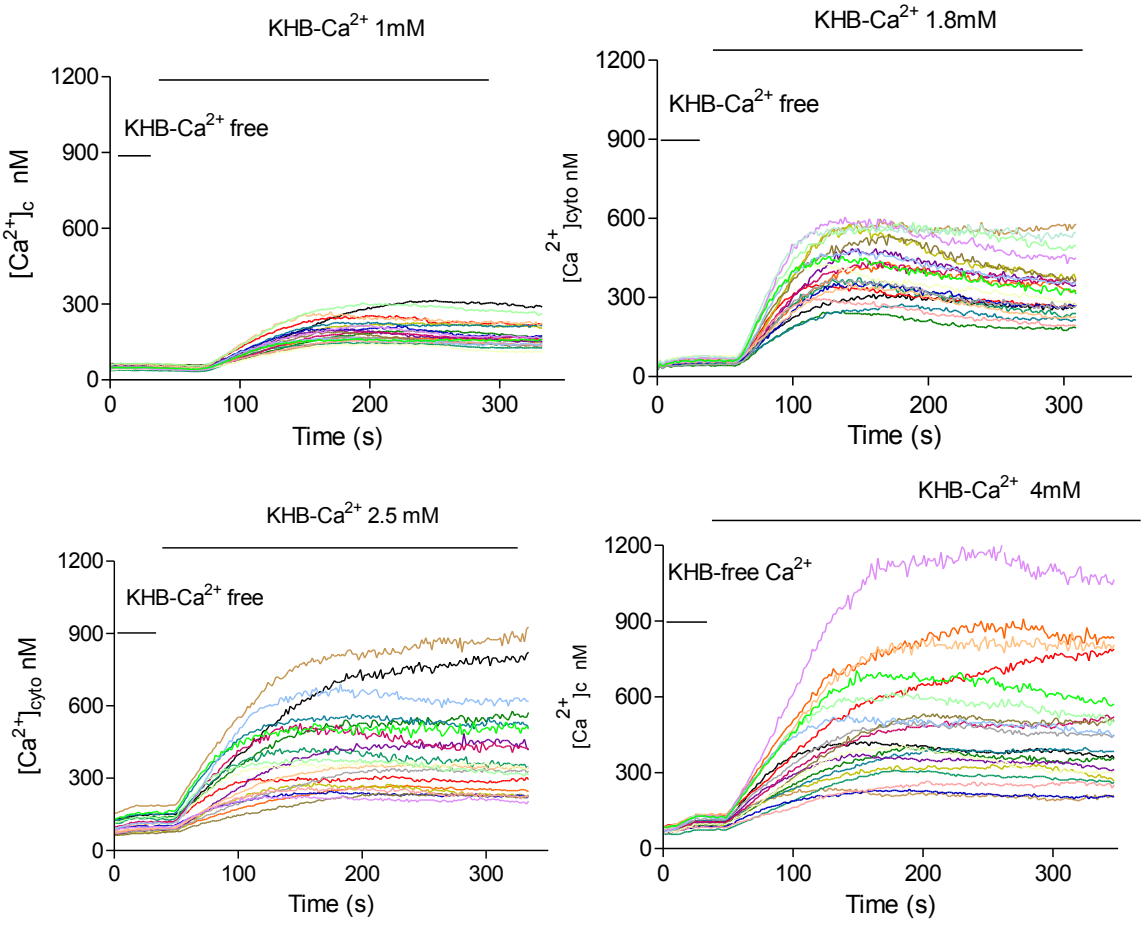

Fig. 3.6. Effect of thapsigargin-induced capacitative Ca^{2+} entry on cytosolic Ca^{2+} signals in SH-SY5Y cells.

Cells loaded with fura-2 (2μM 1h) were pretreated with thapsigargin 5μM for 15-30 min. Cells were perfused with KHB-Ca^{2+} free for the first 30s, then Ca^{2+} added to KHB in different concentration (1, 1.8, 2.5, 4 mM) was added to cells for 5min.

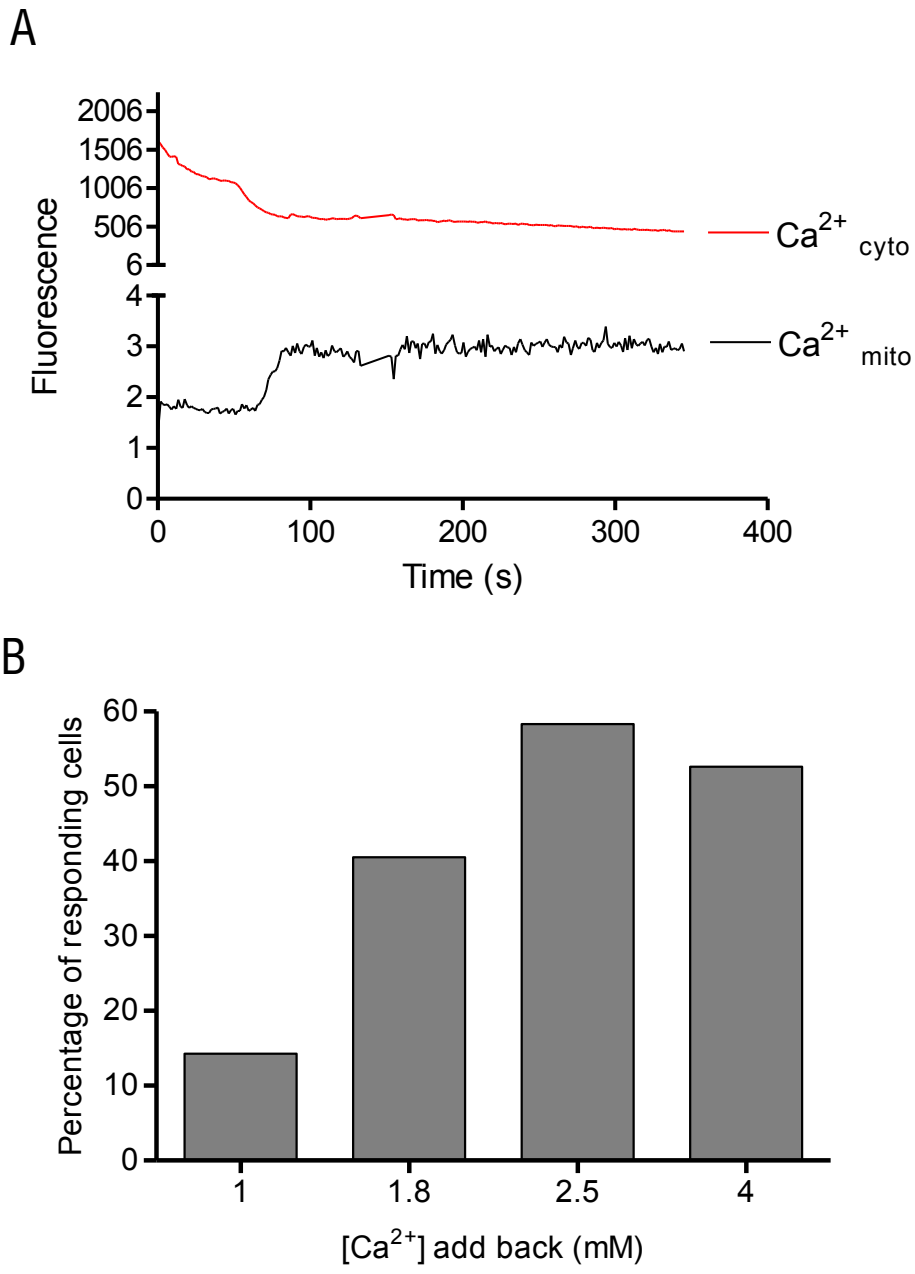

Fig. 3.7. Effect of thapsigargin-mediated capacitative Ca^{2+} entry on mitochondrial Ca^{2+} uptake in control SH-SY5Y cells.

(A) Mitochondrial Ca^{2+} uptake after addition of Ca^{2+} 4mM to thapsigargin pretreated cells. (B) Bar graph of percentage of cells in which mitochondria responded to the addition of Ca^{2+}.

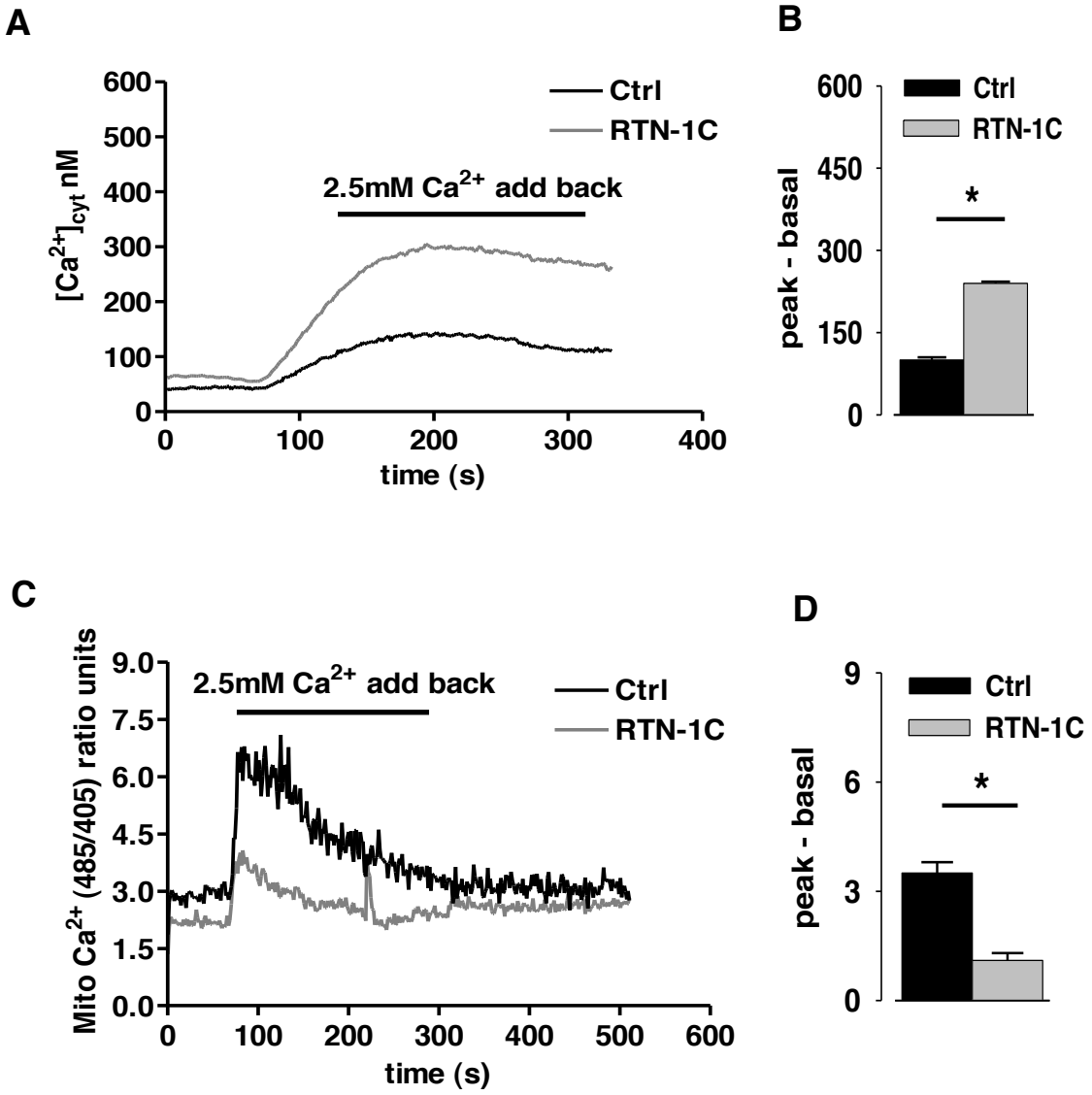

Fig. 3.8. Capacitative Ca^{2+} entry mediated cytosolic and mitochondrial Ca^{2+} signals in RTN1C overexpressing SH-SY5Y cells.

(A) Cells loaded with fura-2 (2μM 1h), were pretreated with thapsigargin 5μM for 15-30 min. Cells were perfused with KHB-Ca^{2+} free for the first 30s , then Ca^{2+} was added to KHB at a concentration of 2.5mM for 5min (B) Quantification of cytosolic peak induced Ca^{2+} responses to Ca^{2+} addition 2.5mM. (C)Cells transfected with 2mtRP were pretreated with the previous protocol described in (A). (D) Quantification of mitochondrial Ca^{2+} responses to Ca^{2+} addition 2.5mM . Unpaired Student's *t*-test, $P<0.05$ for each condition *vs* control. Data are representative of 45 to 50 cells from 4 to 5 experiments.

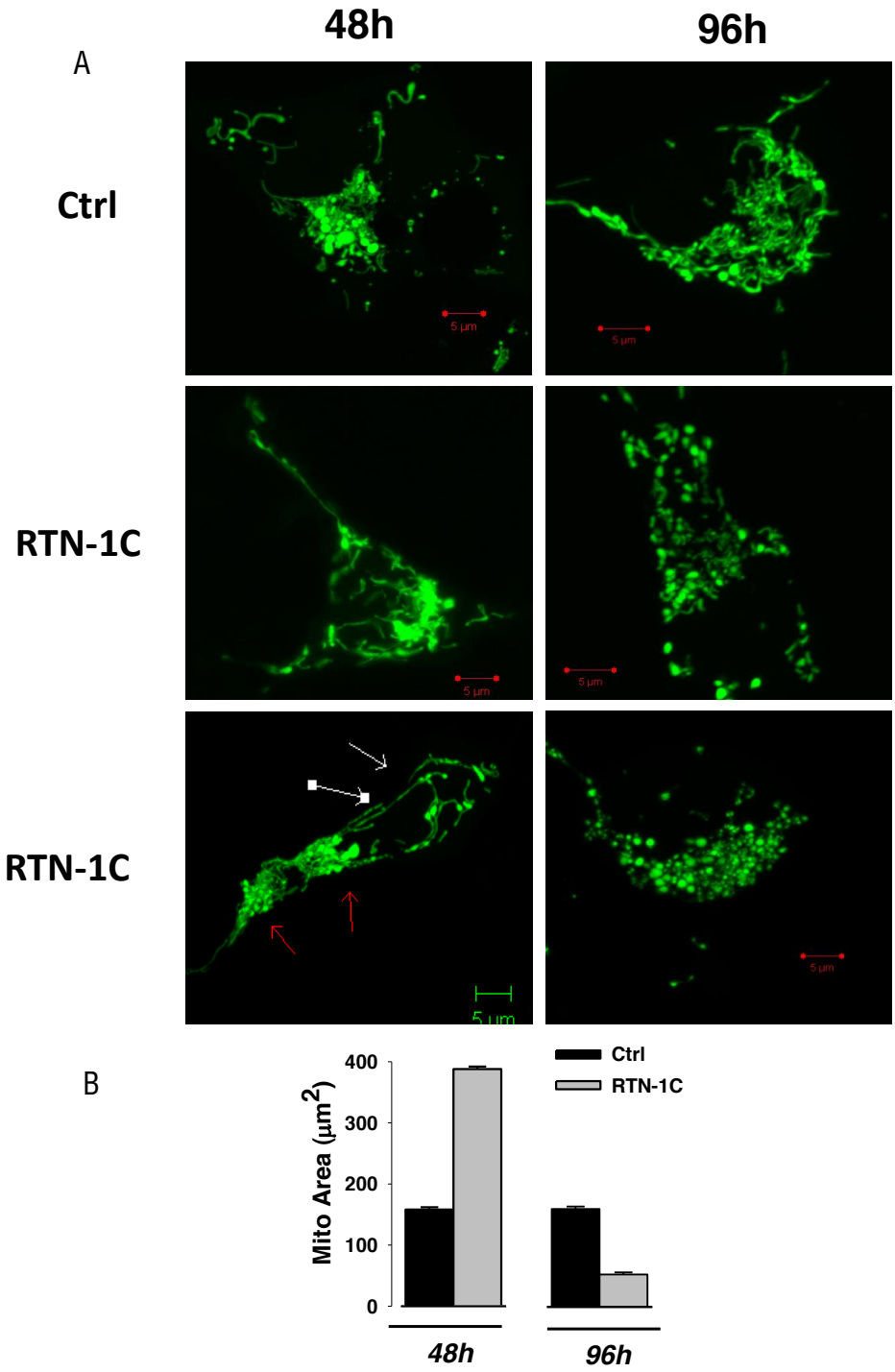

Fig 3.9. RTN1C overexpression induces alterations in mitochondrial morphology. (A) Cells transfected with mito-GFP, were treated with 1 µg/ml doxocycline for 48 and 96 hours. Different mitochondrial phenotyes were imaged by LSM510 confocal microscopy 48h using a x63 objective (plus x4 optical zoom) ,with an optical depth of 1µm. Images of control mitochondria which appear as individual or groups of mitochondrial tubules. In RTN1C cells at 48h, mitochondria show fused and elongated mitochondrial tubules with a more globular structure in the soma of the cells, and long mitochondria in the neurites. At 96h, RTN1C cells display mitochondrial fragmentation and disrupted connectivity of the mitochondrial network. (B). Quantification of mitochonrial area (GFP signal) using Volocity software.

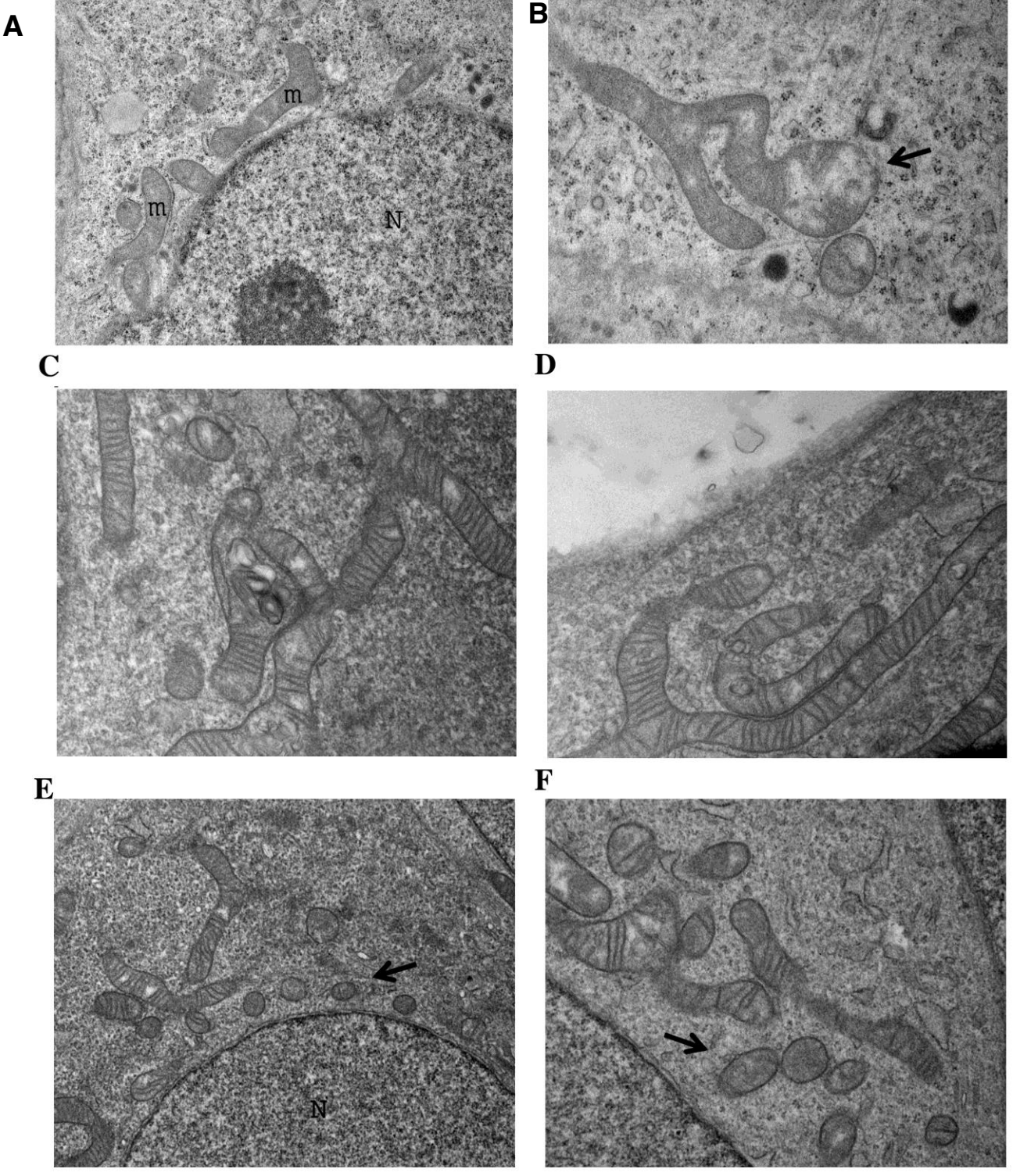

Fig. 3.10. Ultrastructural analysis of SH-SY5Y neurobalstoma cells.
A. The analysis of SH-SY5Y neuroblastoma control cells by electron microscopy shows normal shape mitochondria (m). Nucleus (N). B-D. Cells treated with 1 μg/ml doxocycline for 48 hours. The images show that RTN-1C overexpressing induces the apparence of very elongated and swollen (arrow) mitochondria with dilated cristae. E, F. Cells treated with 1 μg/ml doxocycline for 96 hours. The treatment extension induces mitochondria fragmentation. Numerous mitochondria are visible (arrows). Nucleus (N). Original magnifications: A, E 12.000X, B-D 20.000X F, 20.000X Electron microscopy was done by Dr.Roberta Nardacci at University of Rome Tor Vergata.

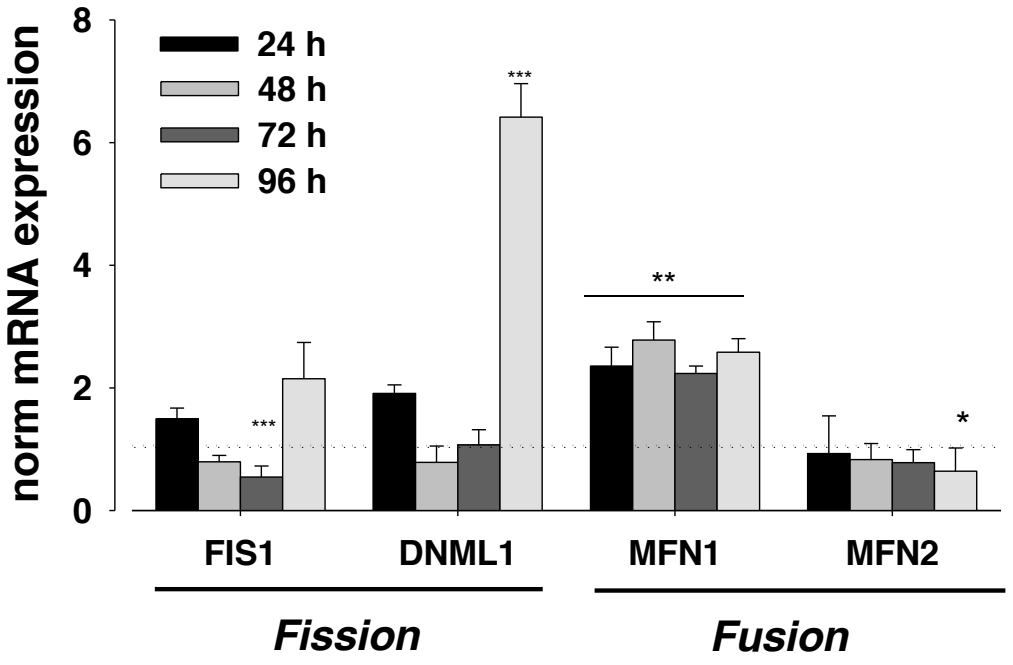

Fig. 3.11. Time-dependent effect of RTN1C overexpression on mitochondrial fission and fusion gene expression.

Real-time quantitative PCR data for SHSY5Y cells and RTN-1C overexpressing cells in response to the 4 different times of induction (24,48,72, and 96 h). The relative mRNA levels of DNM1L , Fis1, MFN1 and MFN 2 are expressed relative to HPRT mRNA level, used as an internal control. Results are means ± SD of three independent determinations.Statistical analysis was performed by Student's t-test, (*). Statistically significant *, $P < 0.05$. **, $P < 0.001$. ***, $P < 0.001$ compared to controls.

Related functions	Symbol	Ref Seq	Description	Normalized mRNA expression			
				Treated sample /control 24h	Treated sample /control 48h	Treated sample /control 72h	Treated sample /control 96h
Mitochondrial fission and fusion	*FIS1*	NM_016068	Fission 1 (mitochondrial outer membrane) homologue (S. cerevisiae)	1.49 (0.15)	0.79 (0.15)	0.54 (0.00015)	2.14 (0.18)
	DNML1	NM_005690	Dynamin 1-like	1.90 (0.07)	0.78 (0.49)	1.06 (0.90)	6.41 (0.002)
	MFN1	NM_033540	Mitofusin 1	2.35 (0.01)	2.78 (0.02)	2.23 (0.06)	2.58 (0.11)
	MFN2	NM_014874	Mitofusin 2	0.92 (0.79)	0.83 (0.49)	0.78 (0.14)	0.64 (0.017)
Housekeeping gene	*HPRT1*	NM_000194	hypoxanthine phosphoribosyltransferase 1	1.00	1.00	1.00	1.00

Table 3.1. Values of time-dependent effect of RTN1C overexpression on mitochondrial fission and fusion gene expression.

Fold change in gene expression was analyzed by the $2^{-\Delta\Delta Ct}$ (see methods for details) of 4 selected genes in treated cells. Data are represented as mean values, n = 9; *p* value treatment *vs* control reported in the brackets.

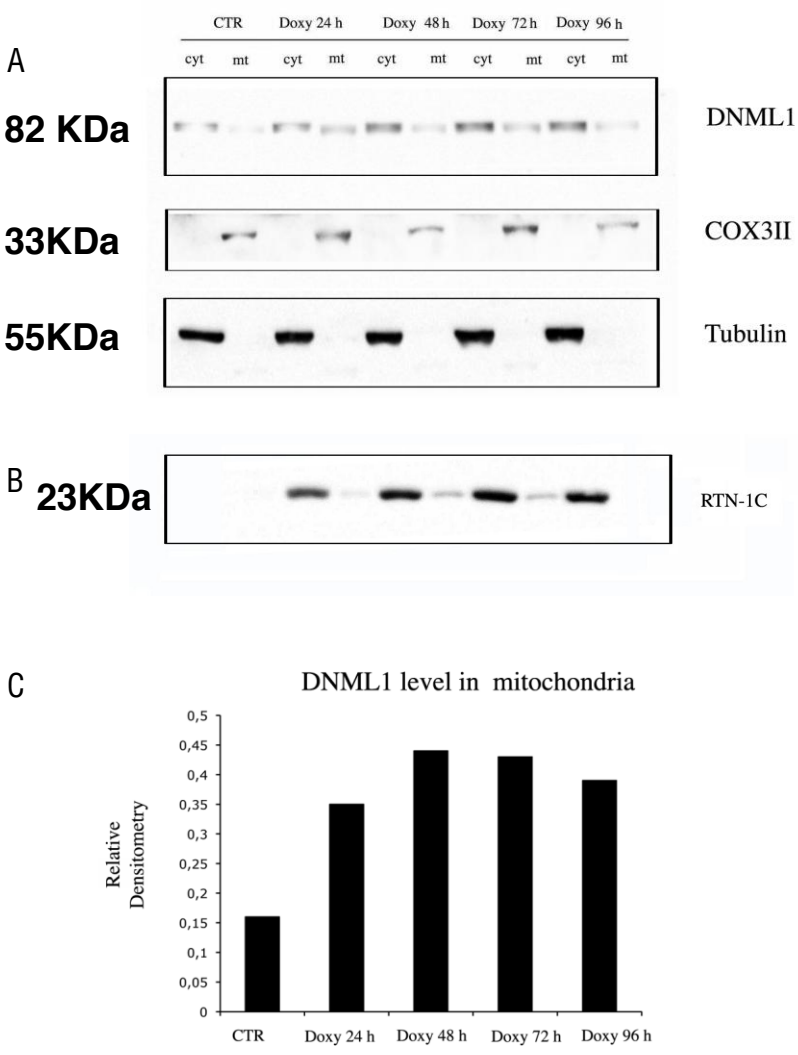

Fig. 3.12. Western blot analysis of DNML1. (A) SH-SY5Y^{RTN-1C} cells were treated with 1 μg/ml doxocycline for the indicated times (24, 48, 72 and 96 hours). Stable cells were lysed, harvested and pelleted, then a fractionation protocol was applied to separate the mitochondrial and cystosolic fractions. Later, western blot analysis was performed on both isolated fractions. Nitrocellulose membranes were probed with an anti-RTN1C (1:1000), anti-DNML1 (1: 1000), and anti-β-tubulin (1:1000), anti- Cox3II (1:2000) were used as loading controls of cytosolic and mitochondrial fractions respectively.(B) RTN1C expression . (C) Densitometric analysis of mitochondrial DNML1 related to Cox3II level. The results shown are representative of three independent experiments.

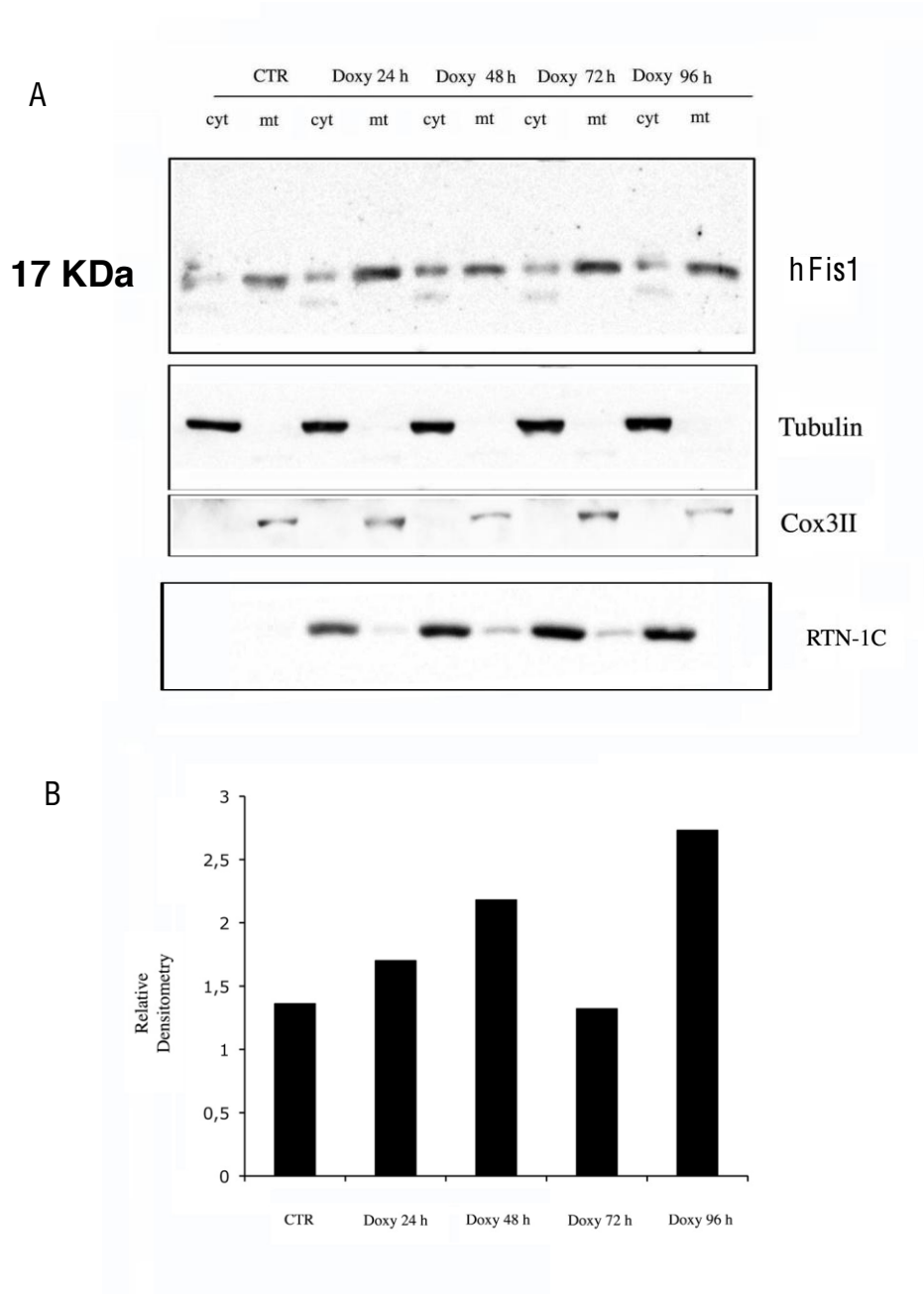

Fig. 3.13. Western blot analysis of hFis1. (A) SH-SY5Y$^{RTN\text{-}1C}$ cells were treated with 1 μg/ml doxocycline for the indicated times (24, 48, 72 and 96 hours). Stable cells were lysed, harvested and pelleted, then a fractionation protocol was applied to separate the mitochondrial and cystosolic fractions. Later, western blot analysis was performed on both isolated fractions. Nitrocellulose membranes were probed with anti-Fis1 (1:500), anti-β-tubulin (1:1000), and anti- OxPhos Complex III core2 subunit antibodies (1:2000) were used as loading controls for cytosolic and mitochondrial fractions respectively. (B) Densitometric analysis of hFis1 related to CIII-Core 2 level. The results shown are representative of three independent experiments.

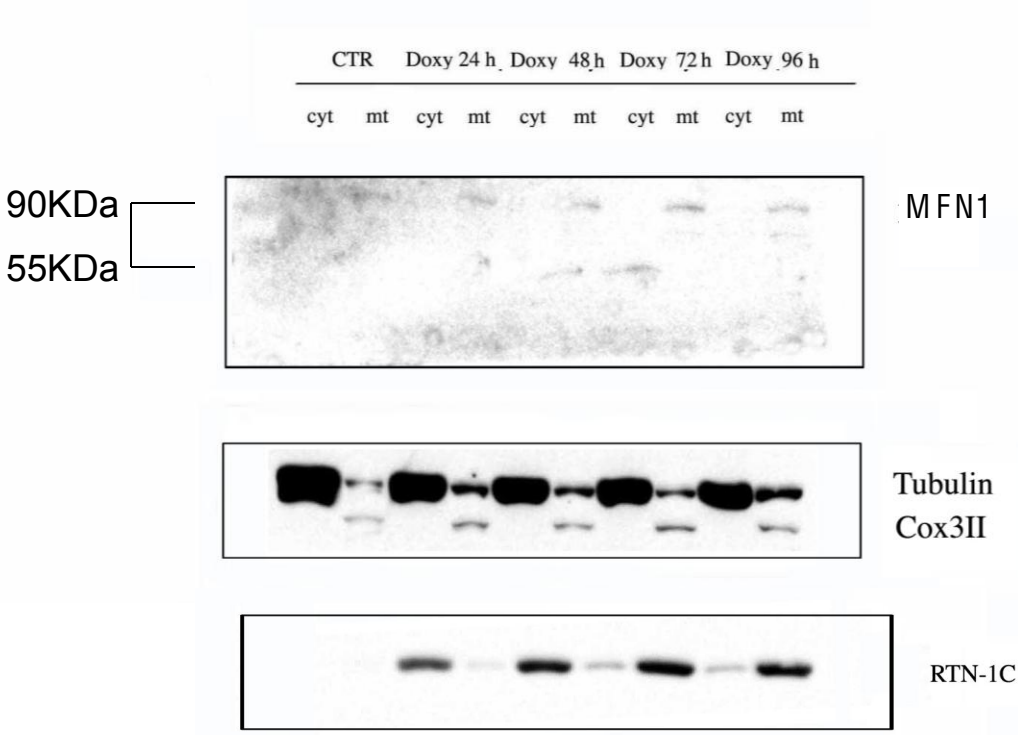

Fig. 3.14. Western blot analysis of MFN1. SH-SY5Y^{RTN-1C} cells were treated with 1 μg/ml doxocycline for the indicated times (24, 48, 72 and 96 hours). Stable cells were lysed, harvested and pelleted, then a fractionation protocol was applied to separate the mitochondrial and cystosolic fractions. Later, western blot analysis was performed on both isolated fractions. Nitrocellulose membranes were probed with an anti-MFN1 (1:500), anti-β-tubulin (1:1000), and anti-Cox3II (1:2000) were used as loading controls for cytosolic and mitochondrial fractions respectively. Data are representative of 3 different experiments

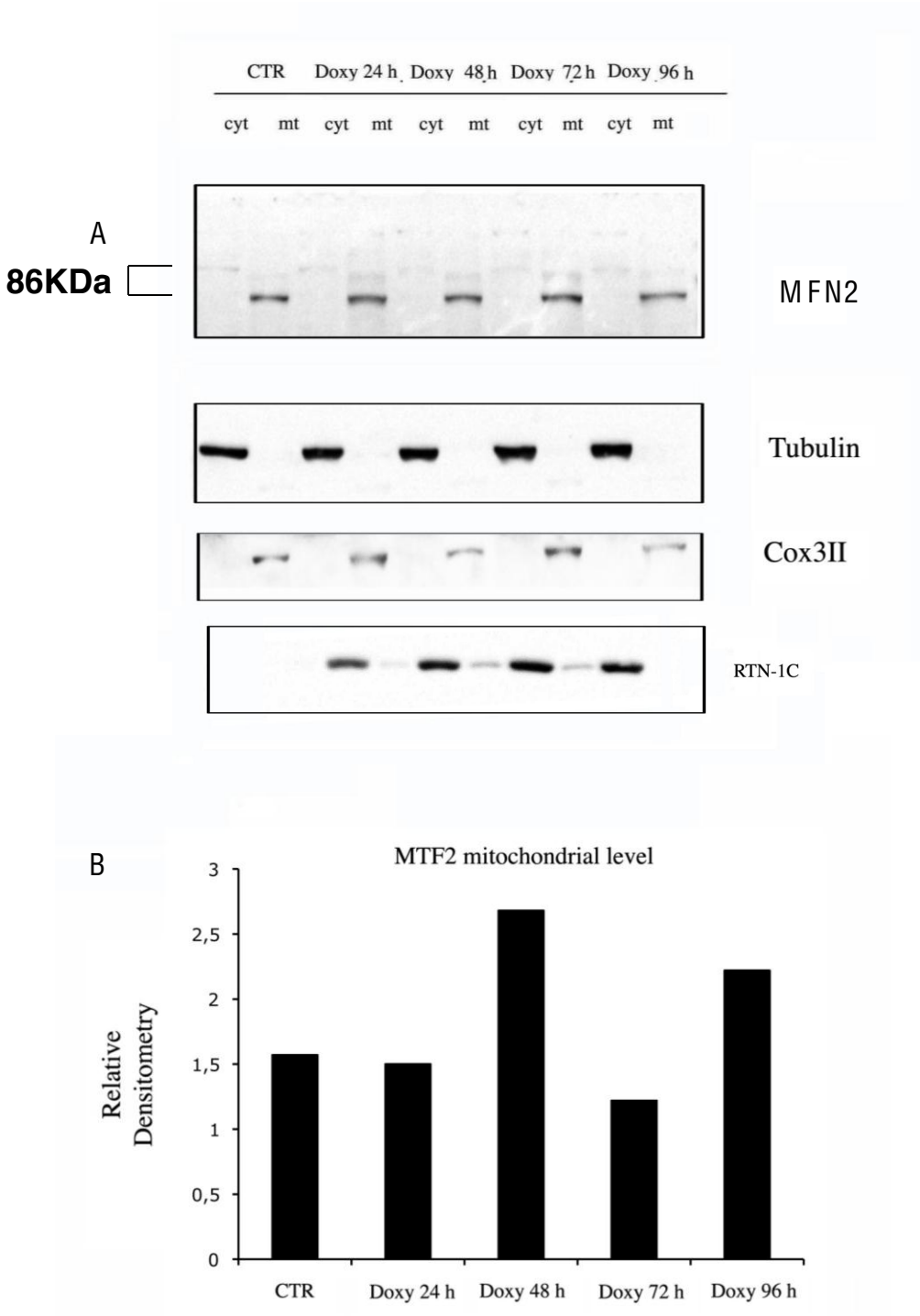

Fig.3.15. Western blot analysis of MFN2. (A) SH-SY5Y^{RTN-1C} cells were treated with 1 μg/ml doxocycline for the indicated times (24, 48, 72 and 96 hours). Mitochondrial and cytosolic fractions were analysed by western blot analysis for MFN2 expression. β-tubulin and CIII-Core 2 were used as loding control of cytosolic and mitochondrial fraction respectively.(B) Densitometric analysis of MFN2 related to CIII-Core 2 level. The results shown are representative of three independent experiments.

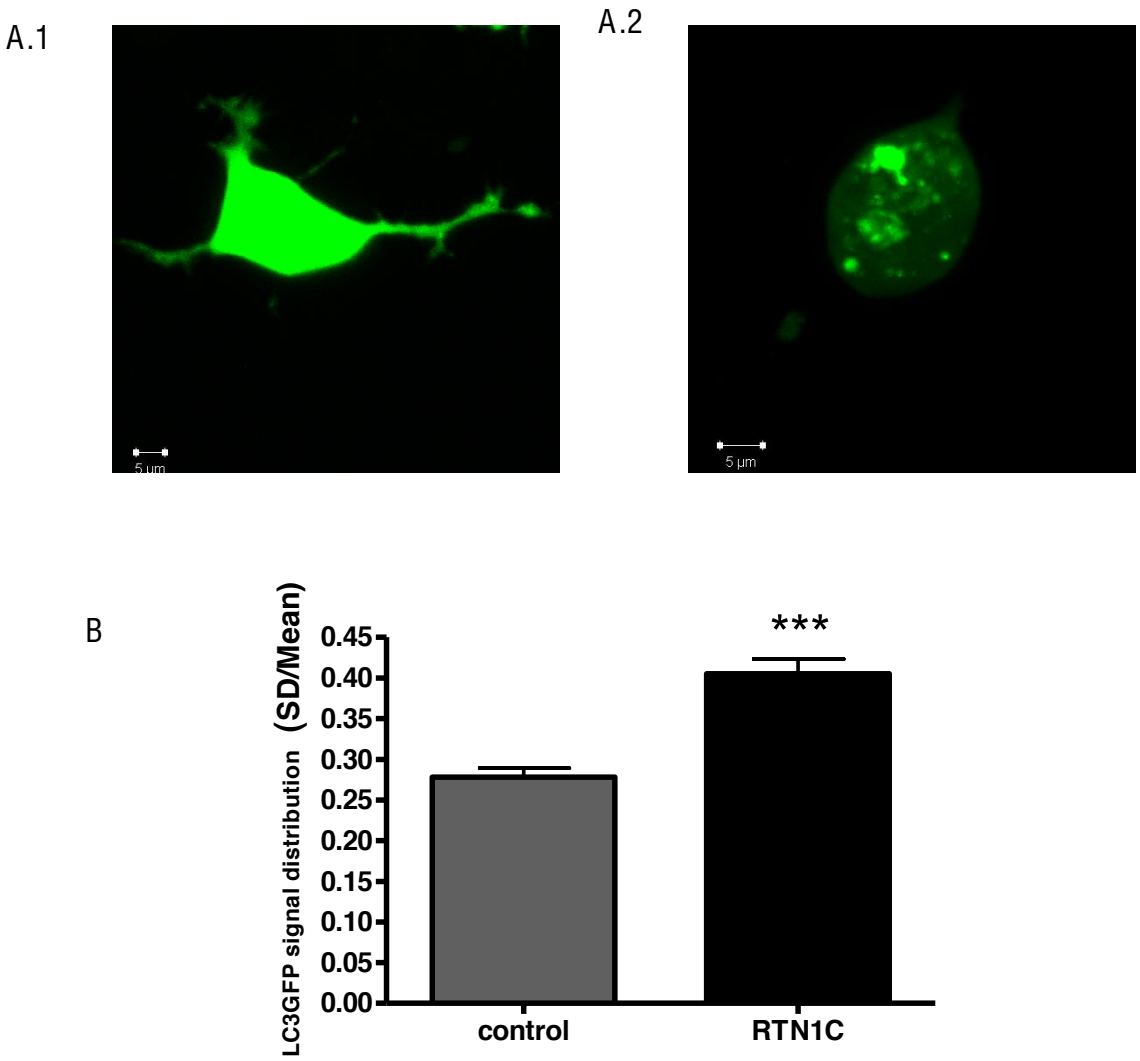

Fig. 4.1. RTN1C overexpression induces autophagy.
SH-SY5Y cells co-transfected with RTN-1C and LC3-GFP for 48h, were analyzed by LSM510 confocal microscopy using a x63 objective (plus x4 optical zoom) ,with an optical depth of 1µm. A.1 shows normal distribution of LC3GFP signal in control cell. A.2 Autophagosome formation appearing as puncta or green dots. (B) Quantification of autophagy in RTN1C cells compared to control. Mean of LC3GPP signal measurements suggest that RTN1C overexpression at 48h induces significant autophagy of which the mean of (SD/ mean) values was (0.40 ± 0.02). Data are representative of 33 cells, compared to control cells which displayed a mean of (0.27 ± 0.01) obtained from 28 cells from 3 experiments for each condition.

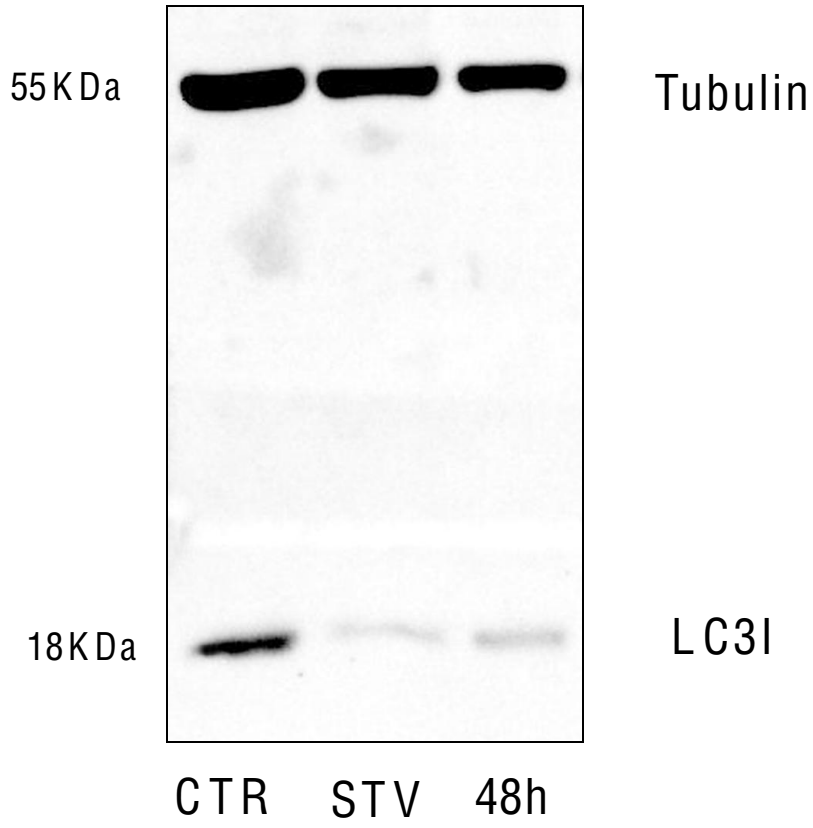

Fig. 4.2. RTN1C overexpression induces autophagy.
Western blot analysis of LC3-I expression in SH-SY5Y neuroblastoma cells starved for 4h (STV) or controls (CTR) and in SH-SY5Y^{RTN-1C} cells treated with 1μg/ml doxocycline for 48 hours. Upper panel shows the β-tubulin expression level as control. The results shown are representative of three independent experiments

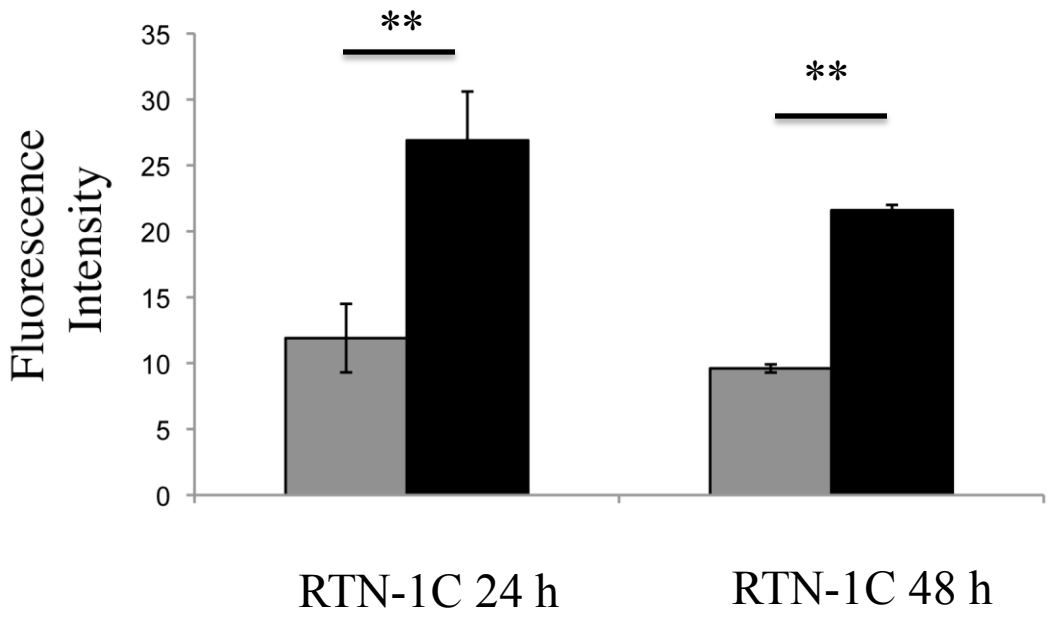

Fig. 4.3. RTN1C overexpression induces acidification of cytoplasm using acridine orange staining.
SH-SY5YRTN-1C cells and SH-SY5Y controls were exposed to 1μg/ml doxycicline for the indicated times, stained with acridine orange and analysed by flow cytometry. Analysis by flow cytometry was done by Paolo Bernardoni at University of Rome Tor Vergata. Results are means ± SD of three independent determinations. (**) Statistically significant ($p < 0.01$) compared to control cells.

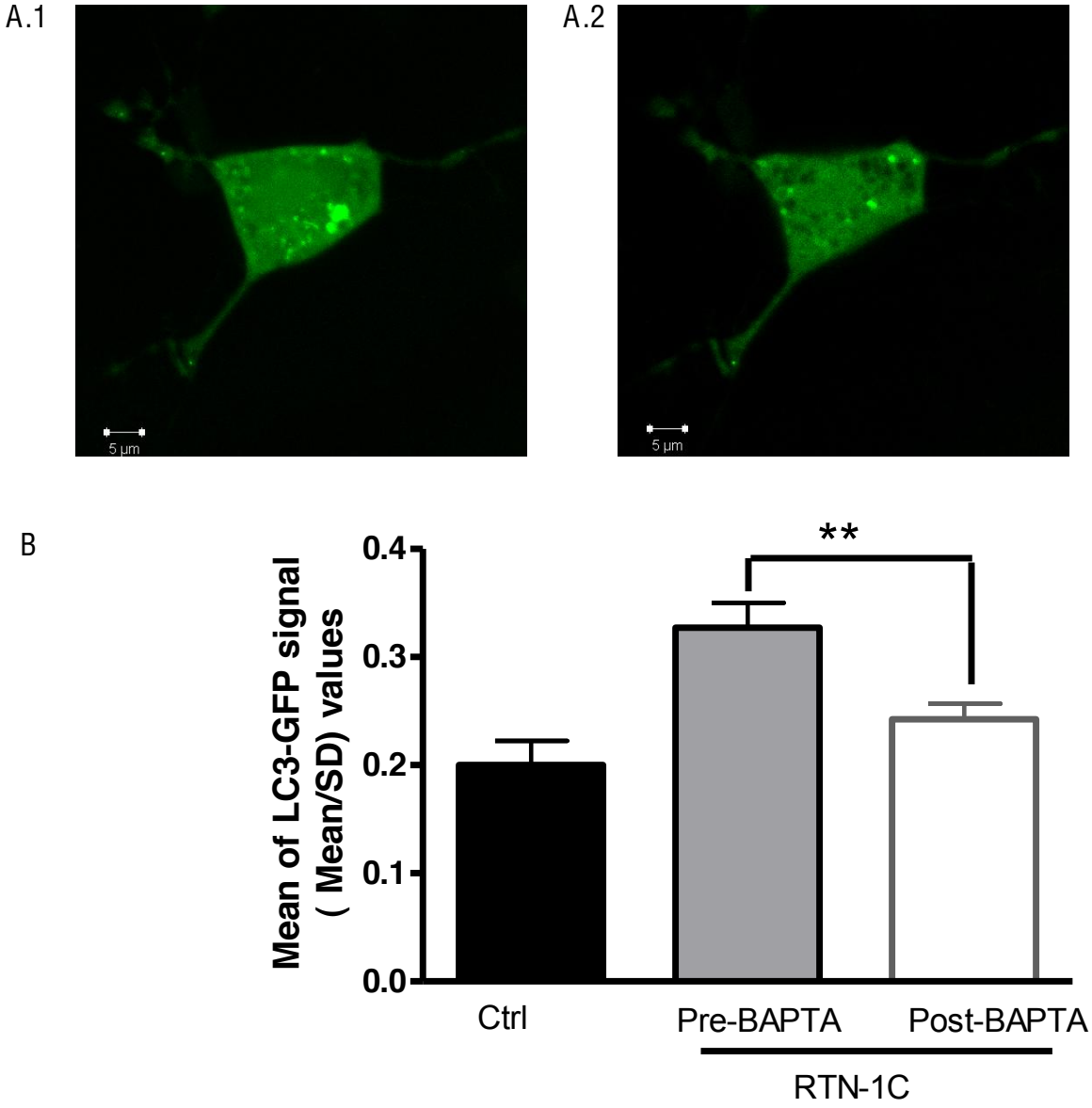

Fig. 4.4. RTN1C-induced autophagy is Ca^{2+} dependent.

SH-SY5Y cells co-transfected with RTN-1C and LC3-GFP for 48h, were analyzed by LSM510 confocal microscopy using a x63 objective (plus x4 optical zoom), with an optical depth of 1µm.(A.1) A representative image of RTN-1C overexpressing cell at 48h, before treatment with BAPTA-AM, where LC3-GFP labeled structures are clearly shown. (A.2) The same cell was treated with BAPTA-AM (5µM, 15 min), which led to a reduction in the number of autophagosomes. (B) Quantification of autophagy where mean of LC3-GFP signal (SD/Mean) values in RTN-1C overexpressing cells pre-BAPTA-AM treatment was (0.32±0.02) and then reduced to (0.24±0.01) following BAPTA-AM administration. Data are representative of 9 cells from 3 experiments, ($P<0.01$).

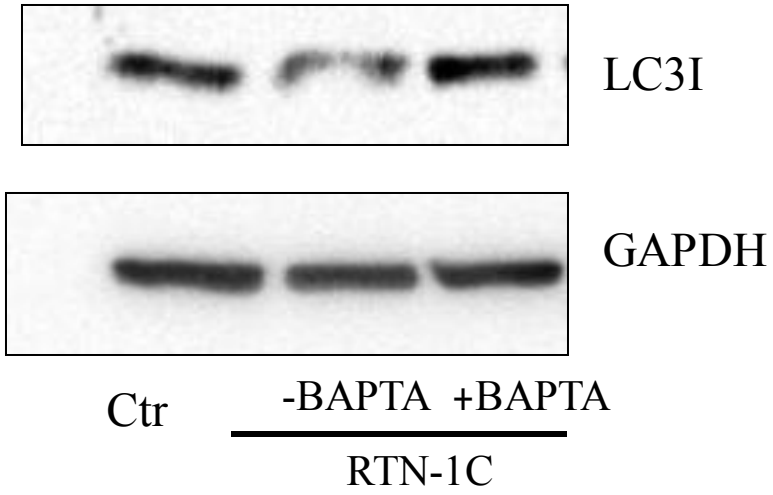

Fig. 4.5. Western blot analysis of LC3I in RTN-1C overexpressing SH-SY5Y cells. SH-SY5Y neuroblastoma cells transiently transfected with RTN-1C construct for 48 hours (RTN-1C), were used for western blot analysis in the presence or absence of BAPTA and controls (Ctr). Nitrocellulose membranes were probed with anti-LC3I, and an anti-GAPDH as a loading control (lower panel). Data are representative of 3 experiments.

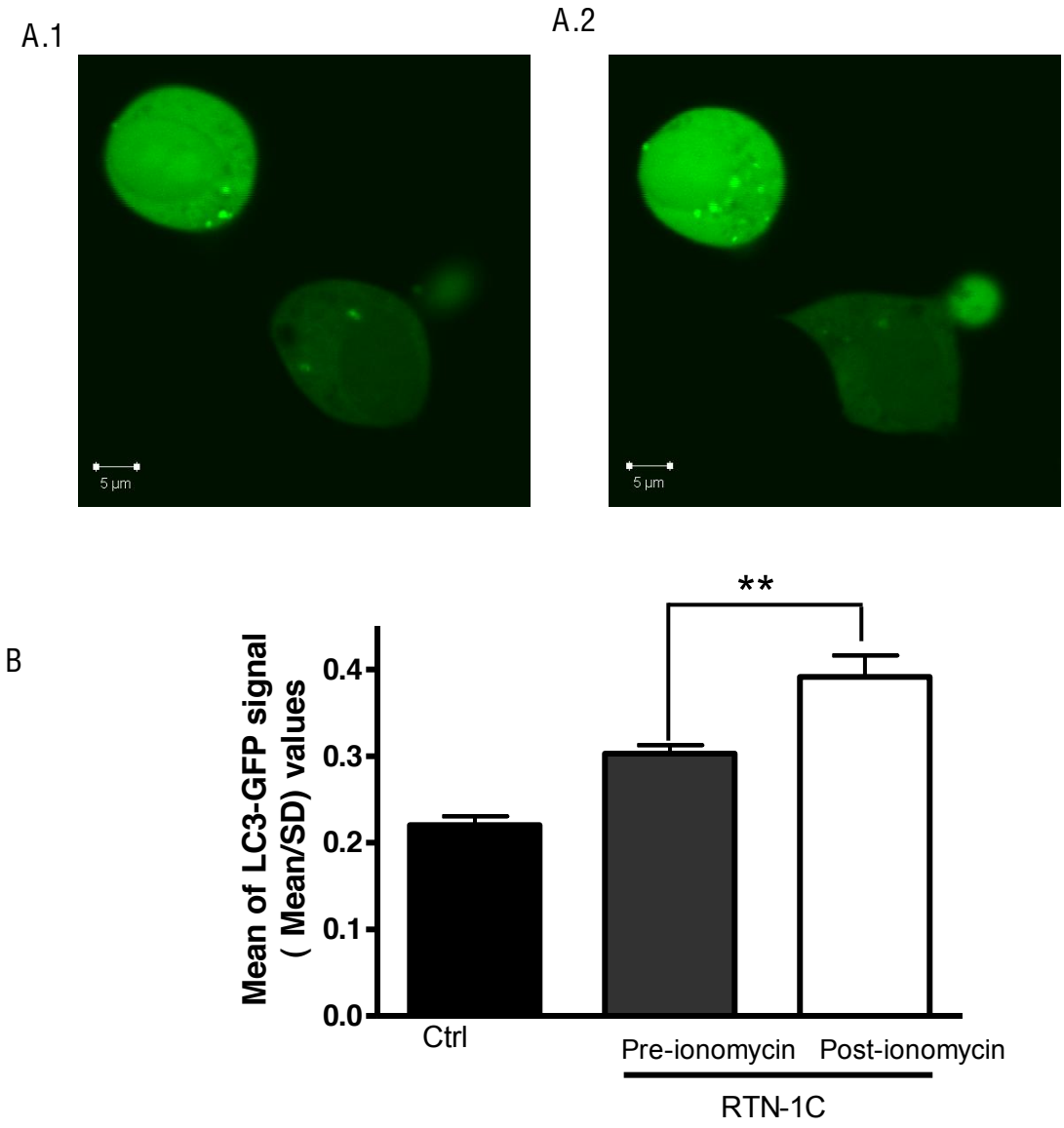

Fig 4.6. RTN1C-induced autophagy is Ca^{2+} dependent. SH-SY5Y cells co-transfected with RTN-1C and LC3-GFP for 48h, were analyzed by LSM510 confocal microscopy using a x63 objective (plus x4 optical zoom), with an optical depth of 1µm.(A.1) A representative image of RTN-1C overexpressing cell at 48h, before treatment with ionomycin, where LC3-GFP labeled structures are clearly shown. (A.2) The same cell was treated with ionomycin (1µM, 5 min), which led to an increase in the number of autophagosomes. (B) Quantification of autophagy in RTN-1C overexpressing cells pre and post treatment of ionomycin compared to control. Mean of LC3-GFP signal (SD/Mean) values was 0.30±0.01 which was increased to 0.40±0.02 post ionomycin administration.Data are representative of 19 cells from 3 experiments, (P<0.01).

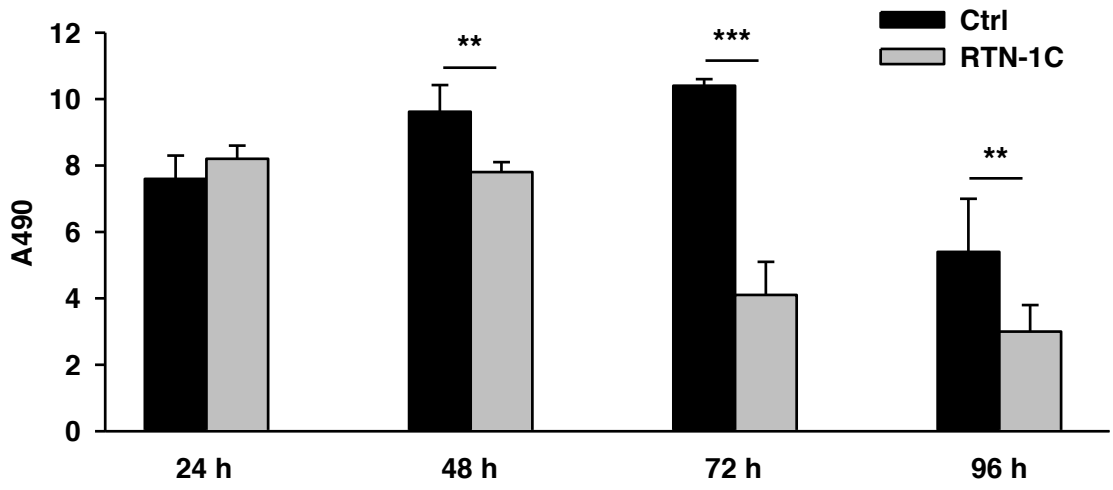

Fig. 4.7. RTN1C overexpression induces cell death.
SH-SY5Y$^{RTN\text{-}1C}$ cells and SH-SY5Y controls were exposed to 1μg/ml doxycycline for the indicated times (24, 48, 72, & 96 h) and used for an MTT assay. Statistically significant (** $p < 0.01$) (*** $p < 0.001$). Statistical test used unpaired Student's t-test.

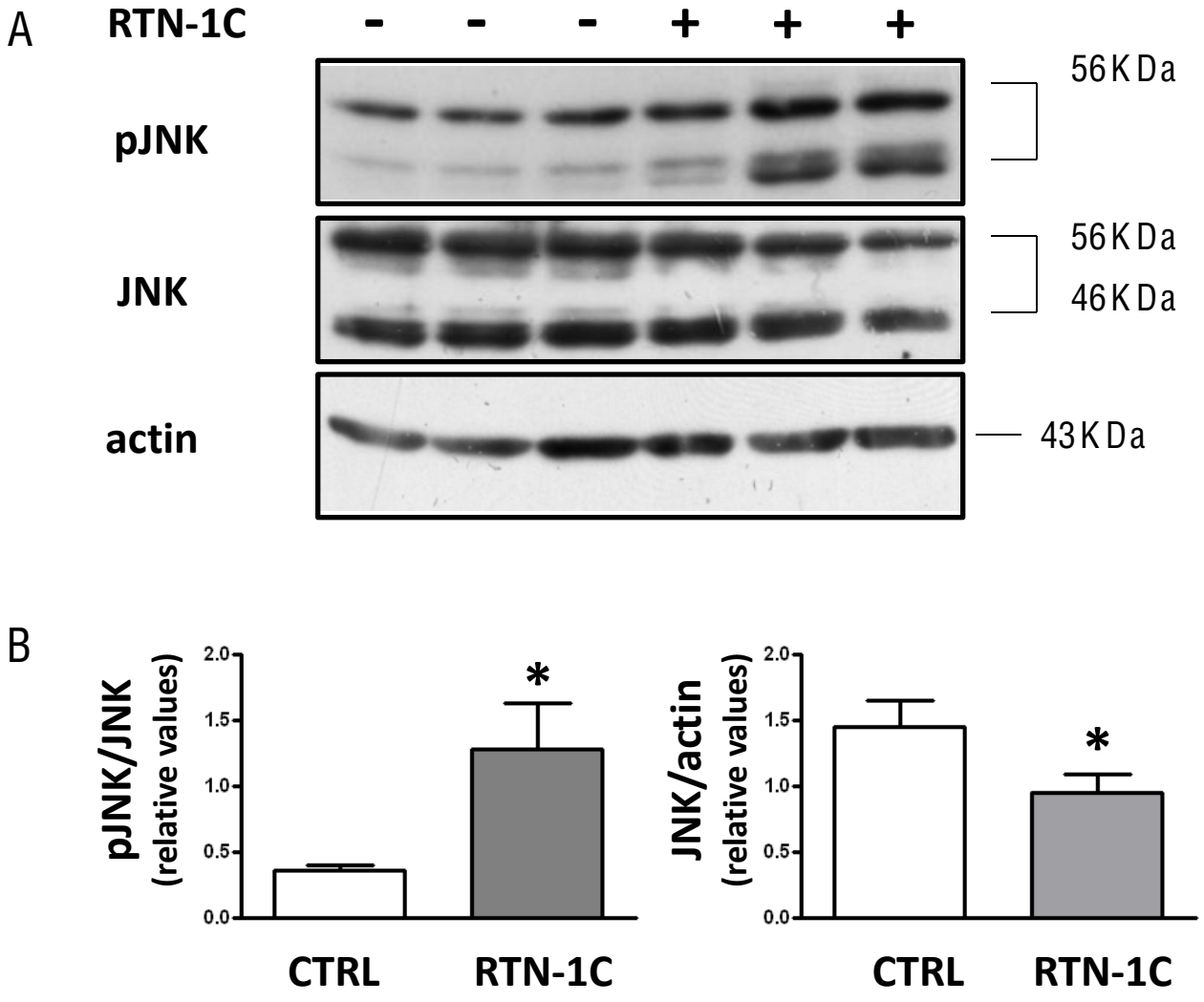

Fig 4.8. RTN-1C overexpression induces JNK phosphorylation in SH-SY5Y at 48h SH-SY5Y cells were transfected with RTN-1C plasmid and lysed after 48. A) Proteins were blotted for different proteins with pJNK, JNK and actin antibodies. B) Densitometric analysis of Western blots where the ratio of pJNK/JNK expresses the phosphorylation of JNK, and ratio of JNK/actin expresses the normalized total JNK protein changes. Data are representative of 3 experiments, $P< 0.05$. Unpaired Student's t-test was applied for statistical analysis. *, $P<0.05$ vs. control.

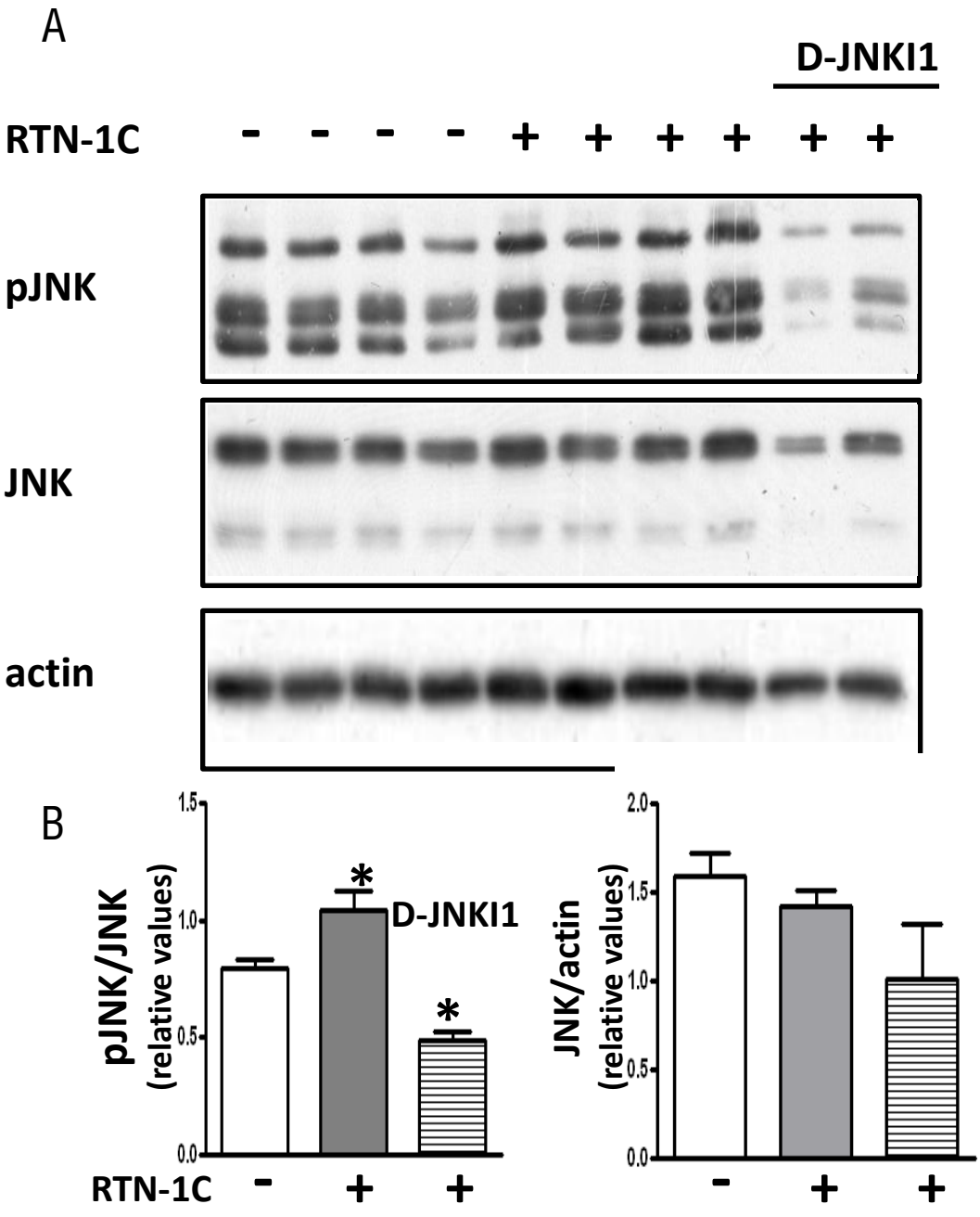

Fig. 4.9. DJNKI1-mediated inhibition of p-JNK in RTN-1C overexpressing cells at 48h.SH-SY5Y cells were transfected with RTN-1C plasmid and lysed after 48, where indicated cells have been treated for 48 hours with D-JNKI1 20μM. A) Membranes were blotted for different proteins with pJNK, JNK and actin antibodies. B) Western blot quantification. Ratio of pJNK/JNK expresses the phosphorylation of JNK. Ratio of JNK/actin expresses the normalized total JNK protein changes. Quantified data from 6 experiments expressed as normalized data on non-phosphorylated protein or actin (mean ± SEM),* $P < 0.05$. ANOVA followed by Tukey's multiple comparison tests were applied for statistical analysis.

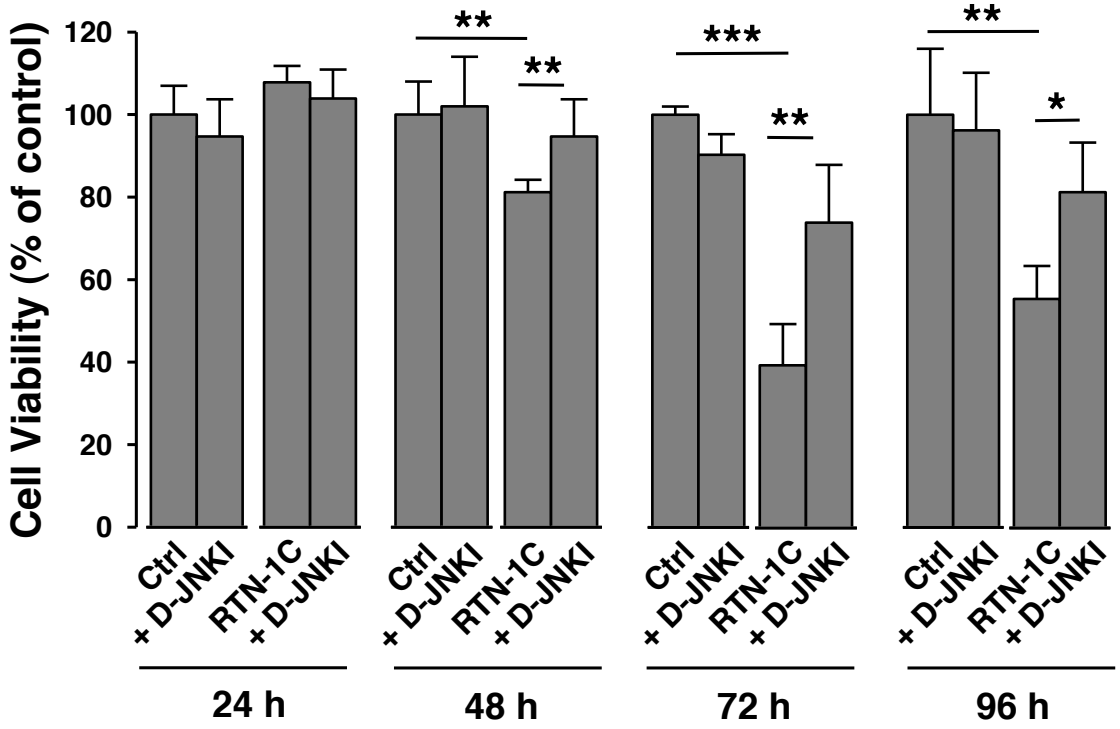

Fig. 4.10. RTN-1C overexpression induces cell death.
SH-SY5Y^{RTN-1C} cells, SH-SY5Y controls, and DJNKI1 treated SH-SY5Y^{RTN1C} cells were exposed to 1μg/ml doxycycline for the indicated times (24, 48, 72, & 96 h), and used for MTT assay. DJNKI1 was administered after RTN-1C induction and left for 24, 48, 72, &96 h). Statistically significant (*$p<0.05$) (** $p<0.01$) (***$p<0.001$). 2-way ANOVA test was applied for statistical analysis.

Gene ID	Gene Symbol and Name	T1	T2
	Calcium-mediated signaling		
10645	**calcium/calmodulin-dependent protein kinase kinase 2, beta**	+	
1236	chemokine (c-c motif) receptor 7	+	
719	complement component 3a receptor 1	+	
84152	**dopamine and camp regulated phosphoprotein, darpp-32**	-	
7462	linker for activation of t cells family, member 2	+	
2847	melanin-concentrating hormone receptor 1	+	
4843	**nitric oxide synthase 2a (inducible, hepatocytes)**	-	-
170685	nudix (nucleoside diphosphate linked moiety x)-type motif 10		-
11163	nudix (nucleoside diphosphate linked moiety x)-type motif 4		-
6261	ryanodine receptor 1 (skeletal)		-
6274	**s100 calcium binding protein a3**	+	+
8877	sphingosine kinase 1	+	
	Apoptosis		
348	apolipoprotein e	+	+
472	ataxia telangiectasia mutated (includes complementation groups a, c and d)		+
10645	**calcium/calmodulin-dependent protein kinase kinase 2, beta**	+	
6347	chemokine (c-c motif) ligand 2	+	
1191	clusterin		+
1026	cyclin-dependent kinase inhibitor 1a (p21, cip1)		+
84152	**dopamine and camp regulated phosphoprotein, darpp-32**	-	
2668	glial cell derived neurotrophic factor		+
8739	harakiri, bcl2 interacting protein (contains only bh3 domain)	+	+
10114	homeodomain interacting protein kinase 3		+
57556	ht018 protein	+	+
3586	interleukin 10	+	
3932	lymphocyte-specific protein tyrosine kinase		+
4804	nerve growth factor receptor (tnfr superfamily, member 16)	+	+
4843	**nitric oxide synthase 2a (inducible, hepatocytes)**	-	-
22822	pleckstrin homology-like domain, family a, member 1	+	+
5777	protein tyrosine phosphatase, non-receptor type 6	+	
6274	**s100 calcium binding protein a3**	+	+
8877	sphingosine kinase 1	+	+
23087	tripartite motif-containing 35	+	
55504	tumor necrosis factor receptor superfamily, member 19		+
7132	tumor necrosis factor receptor superfamily, member 1a		+
	Nervous system development		
3354	5-hydroxytryptamine (serotonin) receptor 1e		-
429	achaete-scute complex-like 1 (drosophila)		-
79026	ahnak nucleoprotein (desmoyokin)	+	+
348	apolipoprotein e	+	+
8938	bai1-associated protein 3		-
10645	**calcium/calmodulin-dependent protein kinase kinase 2, beta**	+	
1129	cholinergic receptor, muscarinic 2		+
1131	cholinergic receptor, muscarinic 3		+
1392	corticotropin releasing hormone		-
51232	cysteine rich transmembrane bmp regulator 1 (chordin-like)		+
84152	**dopamine and camp regulated phosphoprotein, darpp-32**		
1910	endothelin receptor type b		+
84750	fucosyltransferase 10 (alpha (1,3) fucosyltransferase)		+
2637	gastrulation brain homeobox 2		+
2676	gdnf family receptor alpha 3		-
2668	glial cell derived neurotrophic factor		+
2775	guanine nucleotide binding protein (g protein)	+	+
57556	ht018 protein	+	+
5653	kallikrein 6 (neurosin, zyme)		+
4062	lymphocyte antigen 6 complex, locus h		-
4336	myelin-associated oligodendrocyte basic protein		-
4692	needin homolog (mouse)		-
4804	nerve growth factor receptor (tnfr superfamily, member 16)	+	
4804	nerve growth factor receptor (tnfr superfamily, member 16)		+
4762	neurogenin 1	+	
50674	neurogenin 3	+	
4923	neurotensin receptor 1 (high affinity)		-
4815	ninjurin 2	+	
4843	**nitric oxide synthase 2a (inducible, hepatocytes)**	-	-
10178	odz, odd oz/ten-m homolog 1(drosophila)		-
57716	periaxin		-
56126	protocadherin beta 10		-
56126	protocadherin beta 10		-
9771	rap guanine nucleotide exchange factor (gef) 5		+
6197	ribosomal protein s6 kinase, 90kda, polypeptide 3	+	
6274	**s100 calcium binding protein a3**	+	+
11341	scrapie responsive protein 1		+
9723	sema domain, immunoglobulin domain (ig (semaphorin) 3e		-
6505	solute carrier family 1member 1		-
6532	solute carrier family 6 (neurotransmitter transporter, serotonin), member 4		-
30812	sry (sex determining region y)-box 8	+	
9935	v-maf musculoaponeurotic fibrosarcoma oncogene homolog b (avian)		-
9839	zinc finger homeobox 1b		+

Table 5.1. RTN-1C-induced modification in gene expression using cDNA microarray analysis .The genes shown here are those whose expressions are increased (> 2) (+) or decreased (<−2) (−) at 6 h (T1) and 18 h (T2) of induction of experimental conditions. Bold indicated genes investigated further by RT-PCR.Adapted from Fazi et al., (2010).

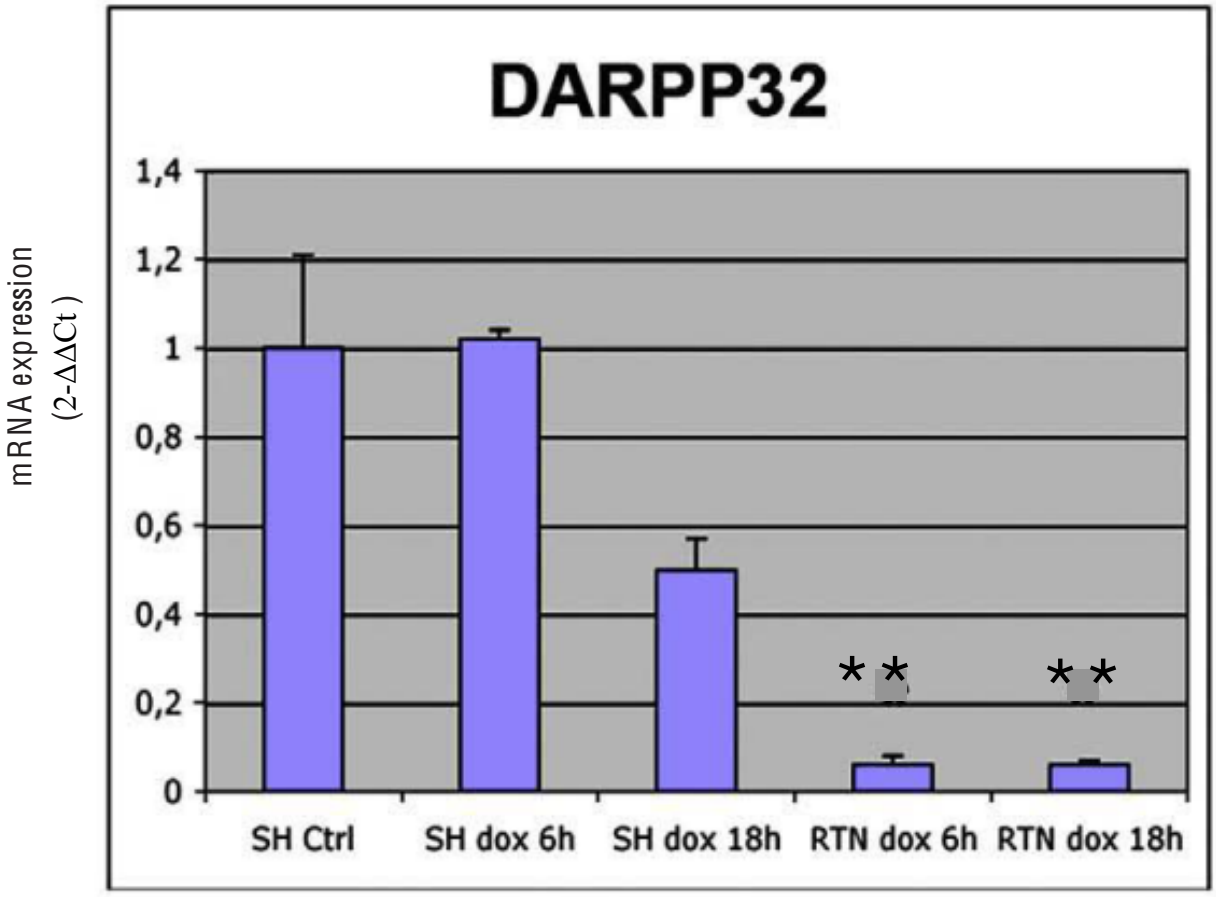

Fig. 5.1. Real-time quantitative PCR data for SH-SY5Y cells and RTN1C overexpressing cells in response to two different induction times (6 and 18 h).

The relative mRNA levels of DARPP-32 are expressed to L34 mRNA level, used as an internal control. SH ctrl cells are SH-SY5Y cells that do not express inducible RTN-1C and were not treated with doxycyline. SH dox are SH-SY5Y cells that do not express inducible RTN-1C and were treated with doxyxyline. RTN dox are SH-SY5Y cells that express inducuble RTN-1C and were treated with doxycyline. Control cells are both SH Ctrl and SH dox 6 h. Results are presented as means±SD of three independent experiments. Statistical analysis was performed by Student's *t* test(*). Statistically significant (p<0.01) compared to control cells.

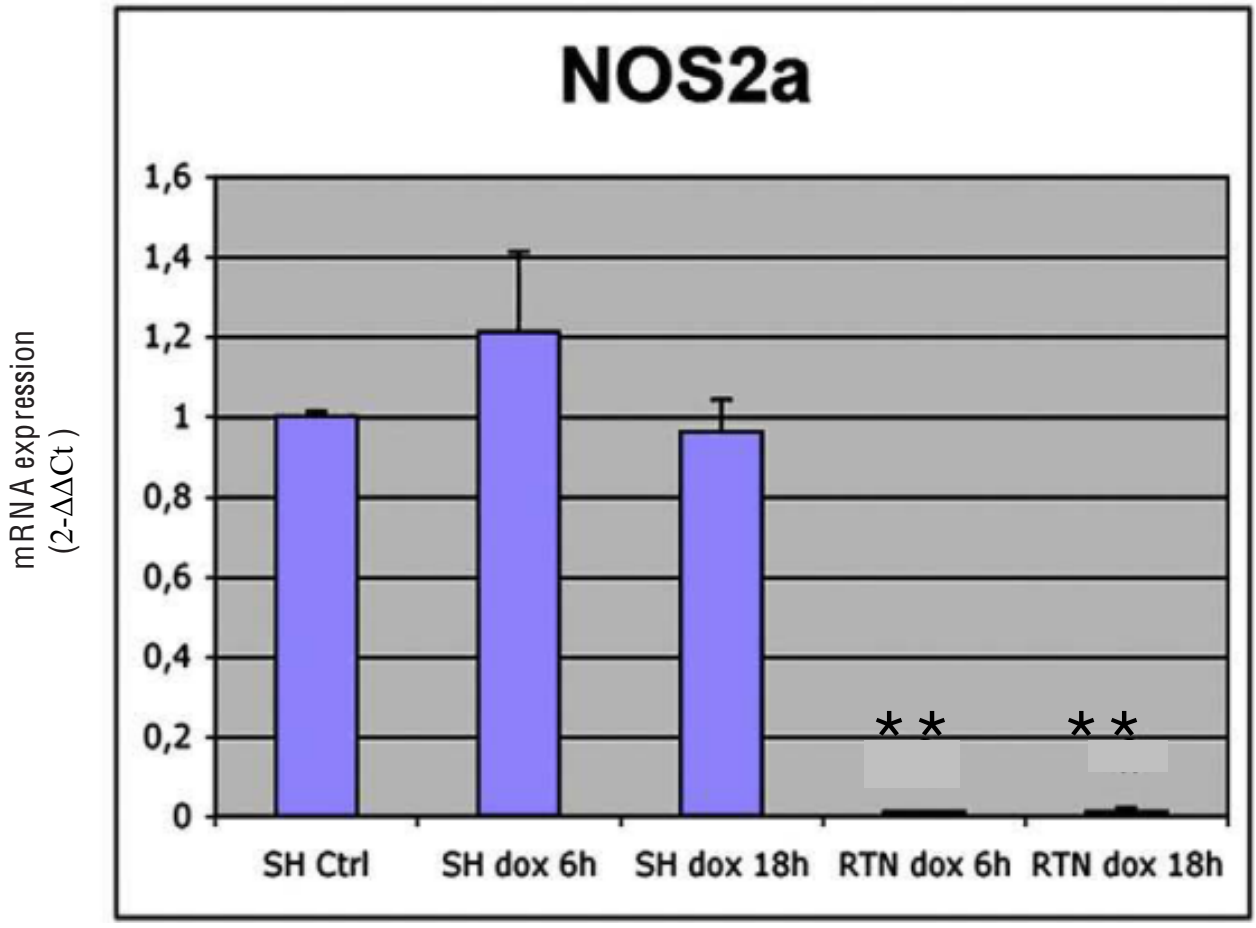

Fig. 5.2. Real-time quantitative PCR data for SH-SY5Y cells and RTN1C overexpressing cells in response to two different induction times (6 and 18 h).

The relative mRNA levels of NOS2a are expressed to L34 mRNA level, used as an internal control. Results are means±SD of three independent experiments. Statistical analysis was performed by Student's *t* test(*). Statistically significant ($p<0.01$) compared to control cells.

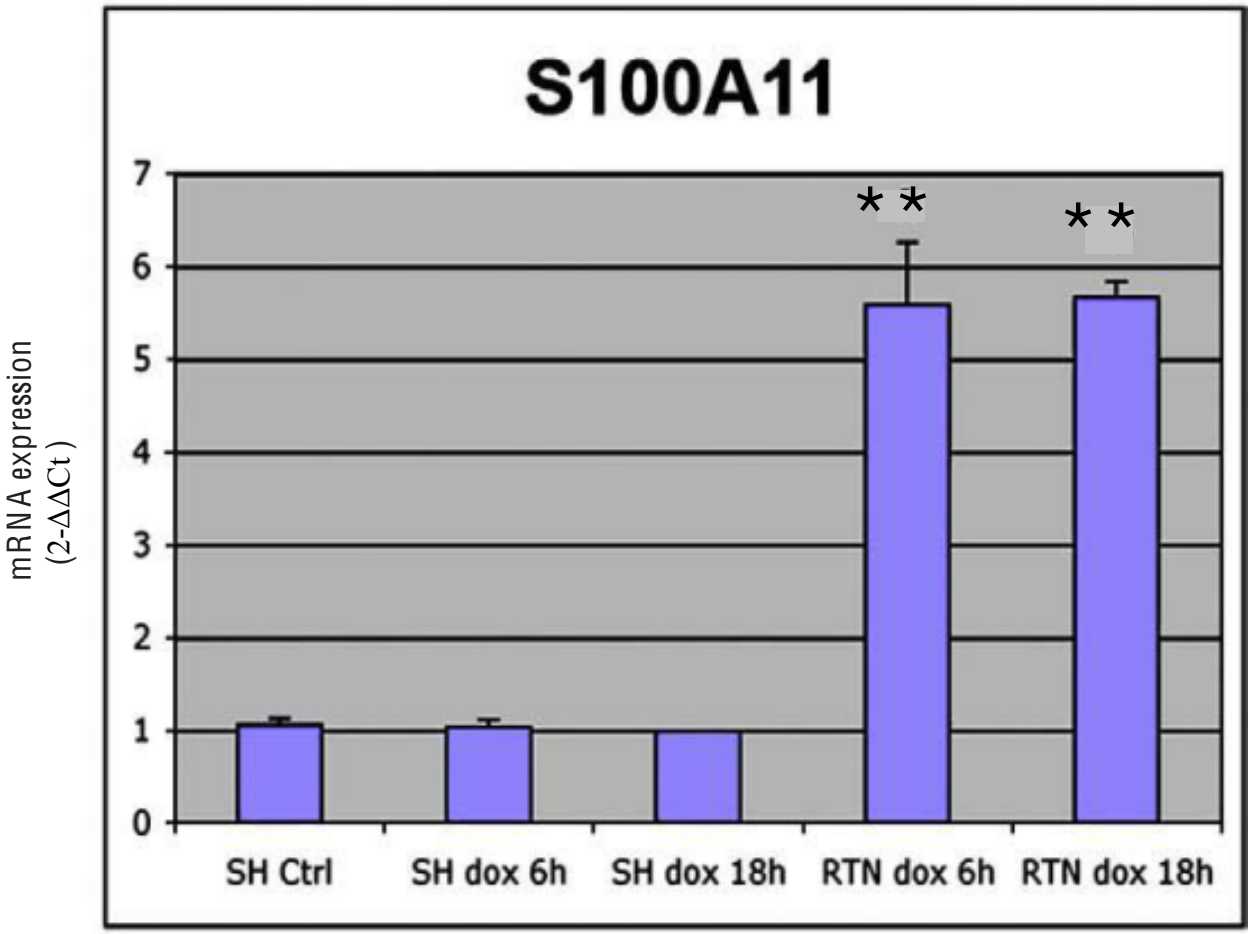

Fig. 5.3. Real-time quantitative PCR data for SH-SY5Y cells and RTN1C overexpressing cells in response to two different induction times (6 and 18 h).

The relative mRNA levels of S100A11are expressed to L34 mRNA level, used as an internal control. Results are means±SD of three independent experiments. Statistical analysis was performed by Student's *t* test(*). Statistically significant ($p<0.01$) compared to control cells.

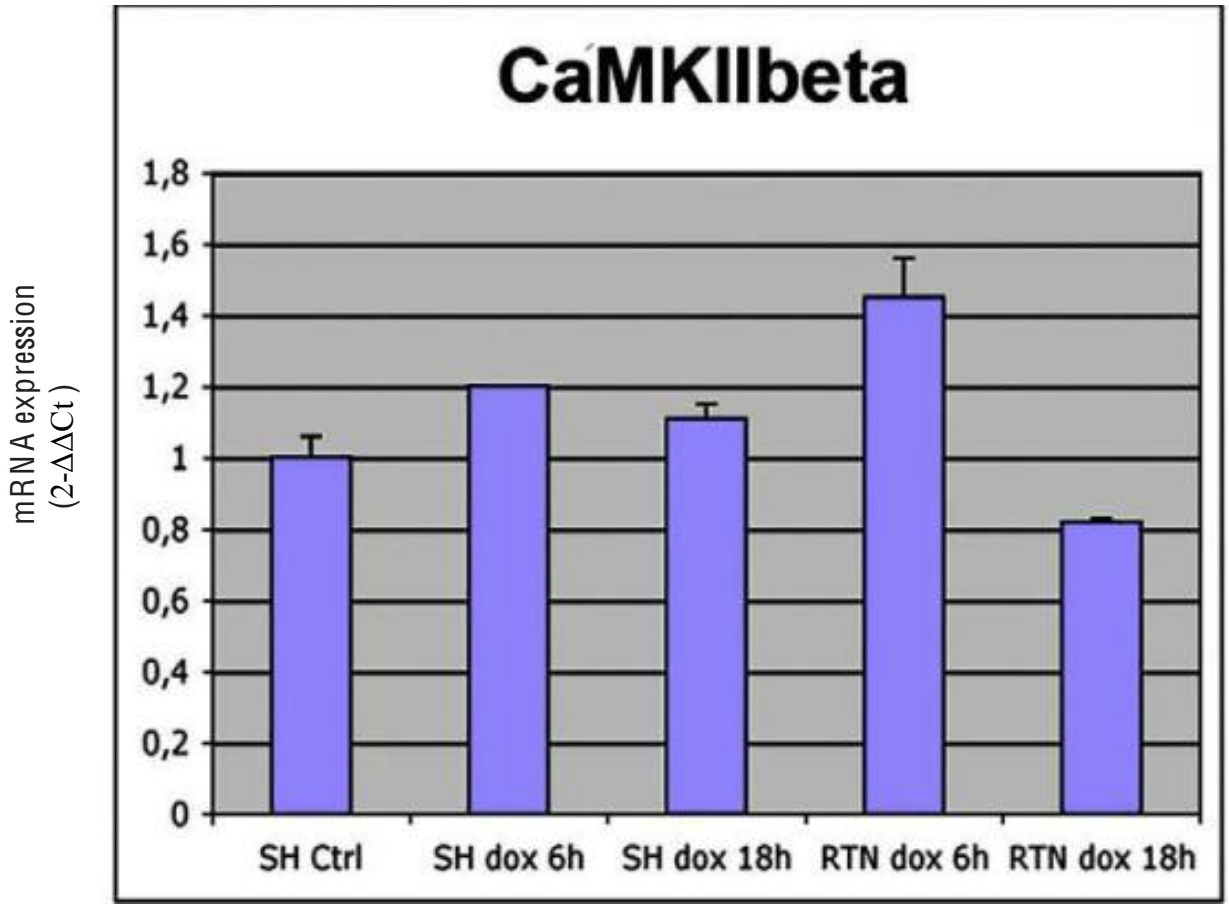

Fig. 5.4. Real-time quantitative PCR data for SH-SY5Y cells and RTN1C overexpressing cells in response to two different induction times (6 and 18 h).

The relative mRNA levels of CaMKIIbeta are expressed to L34 mRNA level, used as an internal control. Results are means±SD of three independent experiments. Statistical analysis was performed by Student's *t* test.

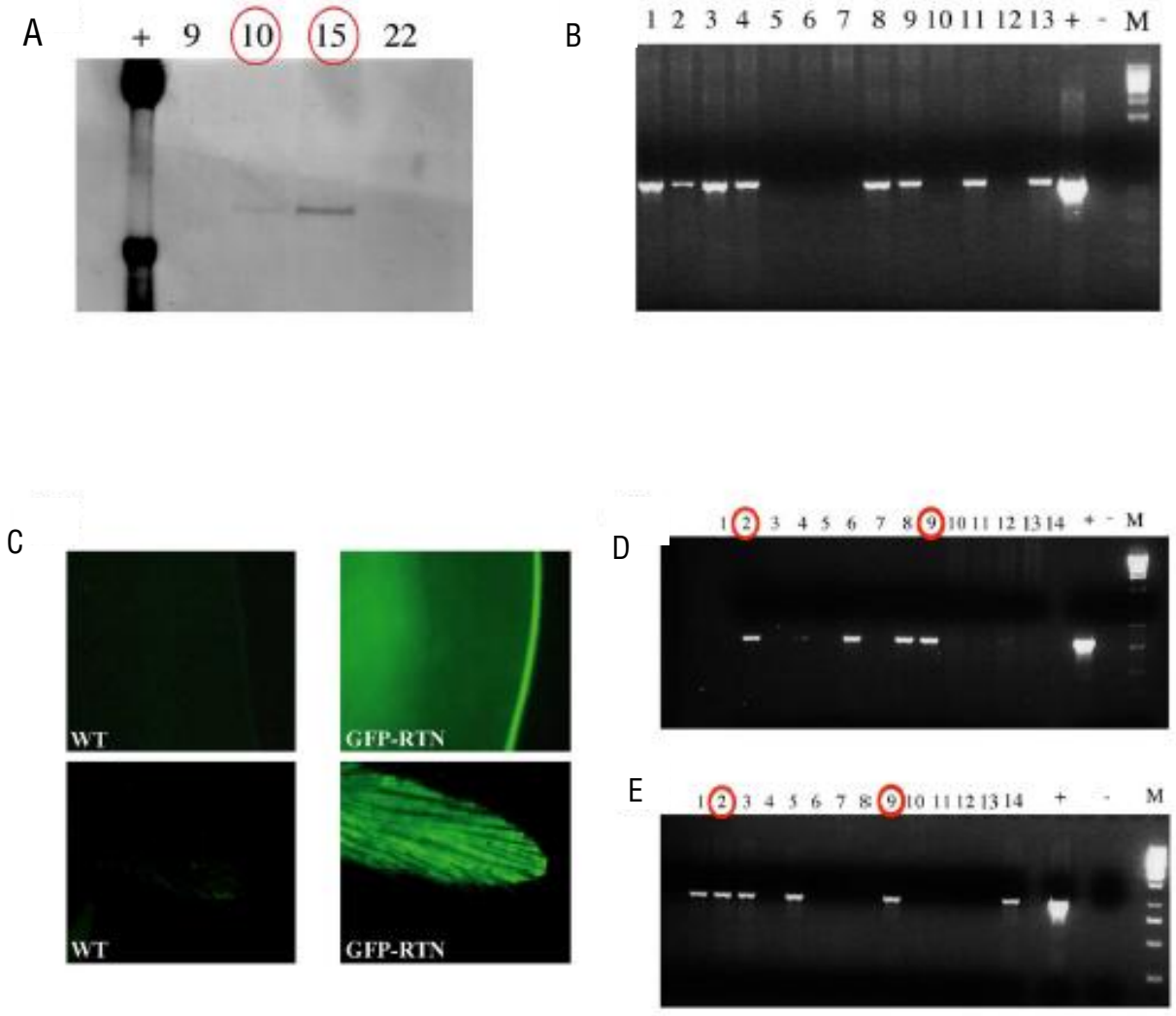

Fig. 5.5. Generation and characterization of transgenic mouse. (A) Southern blot analysis of genomic DNA of transgenic mice number 9, 10, 15, 22 digested with Bgl II enzime. Numbers ringed in red are the positive line. (B) Representative PCR to identify the presence of RTN-1C cDNA in fourteen transgenic GFP/RTN-1C mice. (C) Analysis of GFP expression by fluorescence microscopy in tail and brain sections of Wt and GFP-RTN-1C transgenic mice. Mouse strain is c57bl 6j. Full phenotype characterization of this novel transgenic model is currently under evaluation. (D,E) Representative PCR to identify the presence of CRE gene (D) and RTN-1C gene (E) in fourteen transgenic Cre+/RTN-1C+ mice. The numbers ringed in red are the mice positive for both PCR. Adapted from Fazi et al., (2010)

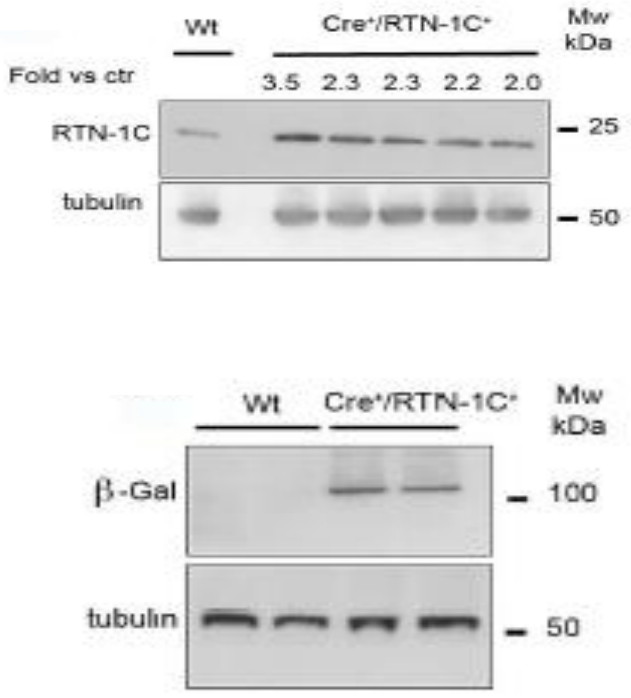

Fig. 5.6. Western blot analysis of RTN-1C and β-Gal in RTN-1C transgenic mice *vs.* wild type animals. RTN-1C and β-Gal expression in cerebral cortex obtained from Wt and Cre+/ RTN-1C+ transgenic mice. Numbers indicate quantitative analysis of RTN-1C expression levels of which 50μg of protein sample was loaded. Control samples are obtained from wild type mice.

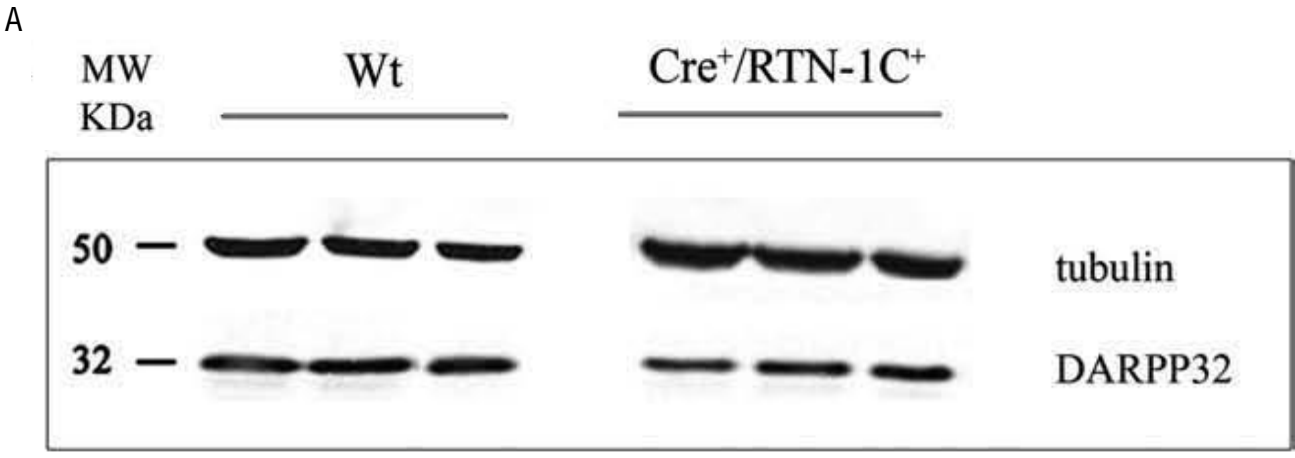

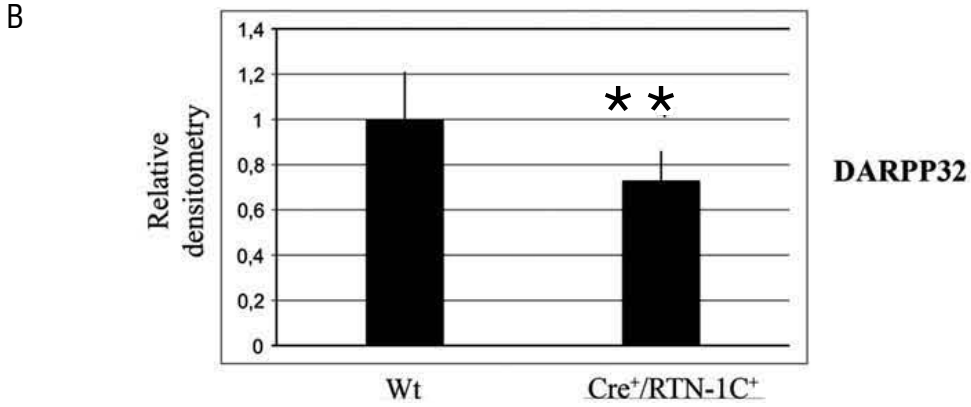

Fig. 5.7. Western blot (A) and densitometric analysis (B) of DARPP-32 related to tubulin protein expression level in Wt and Cre+/RTN-1C+ transgenic mice. 50μg of protein samples was load taken from brain cortices. Results are means ± SD of three independent determinations. Statistical analysis was performed by Student's *t*-test, (**) Statistically significant ($p < 0.01$) compared to control cells.

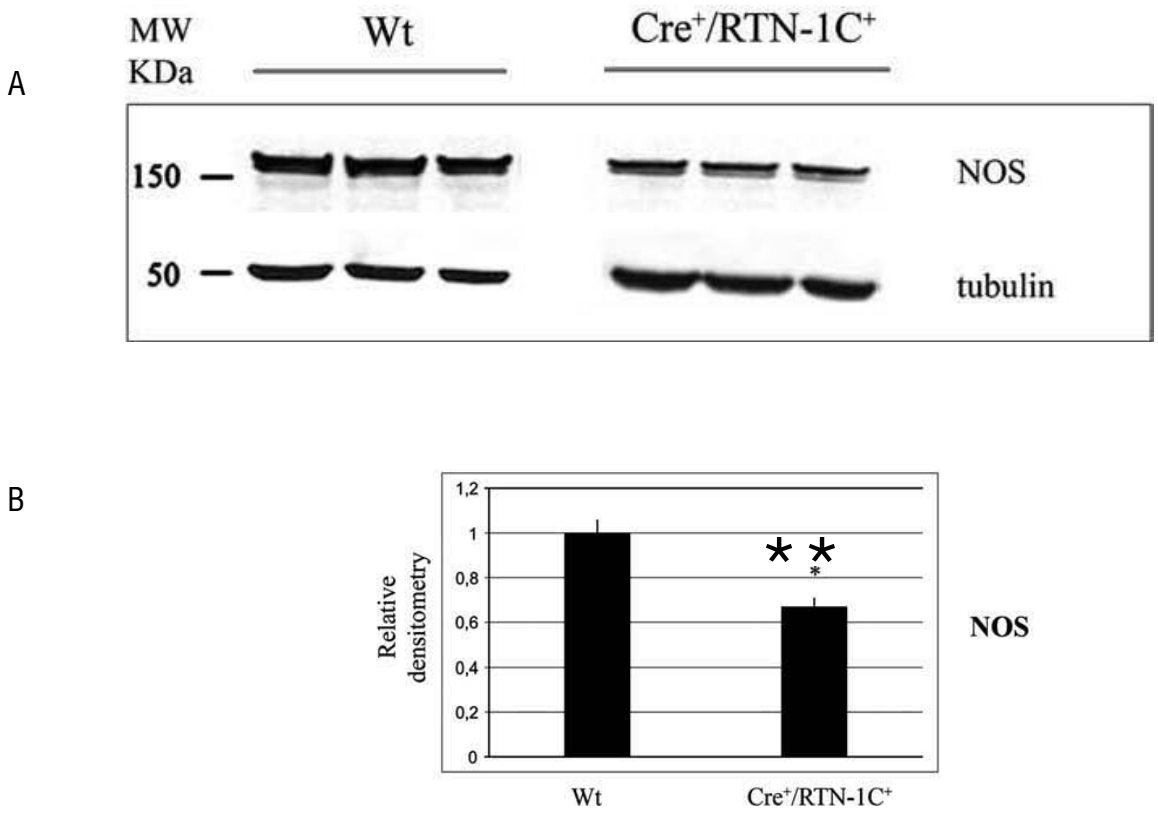

Fig. 5.8. Western blot (A) and densitometric analysis (B) of NOS related to tubulin protein expression level in Wt and Cre+/RTN-1C+ transgenic mice. 50μg of protein samples was load taken from brain cortices. Results are means ± SD of three independent determinations. Statistical analysis was performed by Student's *t*-test, (**) Statistically significant ($p < 0.01$) compared to control cells.

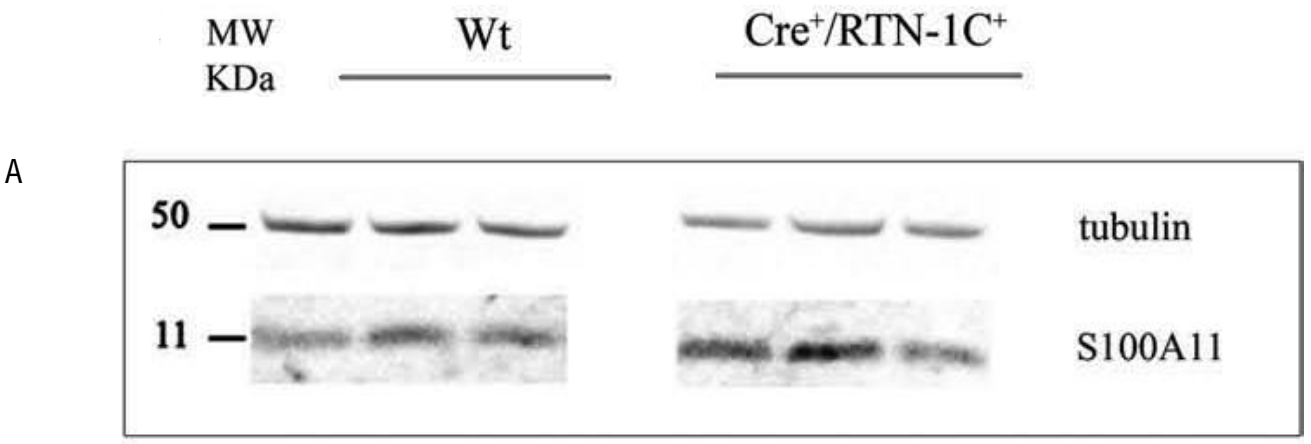

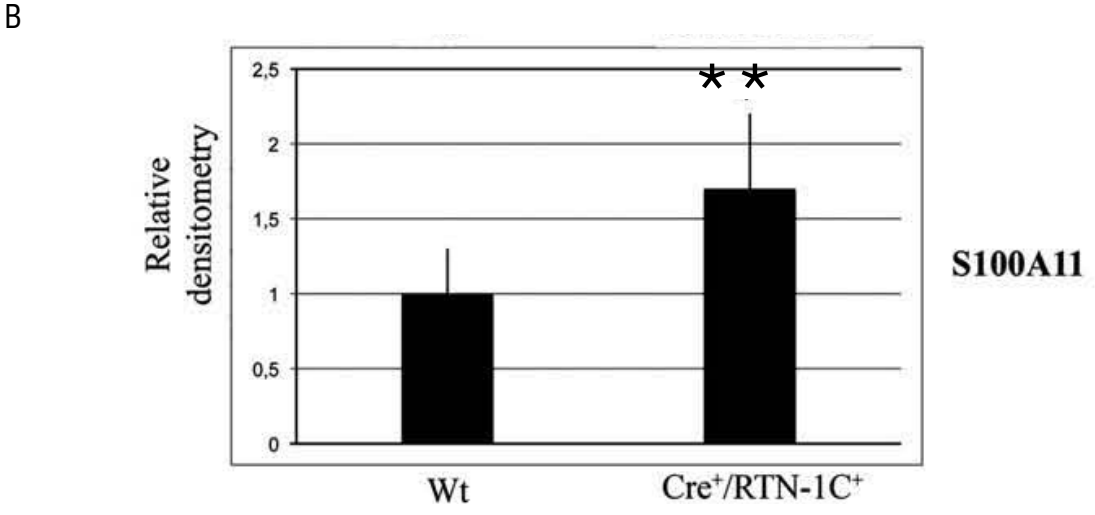

Fig. 5.9. Western blot (A) and densitometric analysis (B) of S100A11 related to tubulin protein expression level in Wt and Cre+/RTN-1C+ transgenic mice. 50μg of protein samples was load taken from brain cortices. Results are means ± SD of three independent determinations. Statistical analysis was performed by Student's *t*-test, (**) Statistically significant ($p < 0.01$) compared to control cells.

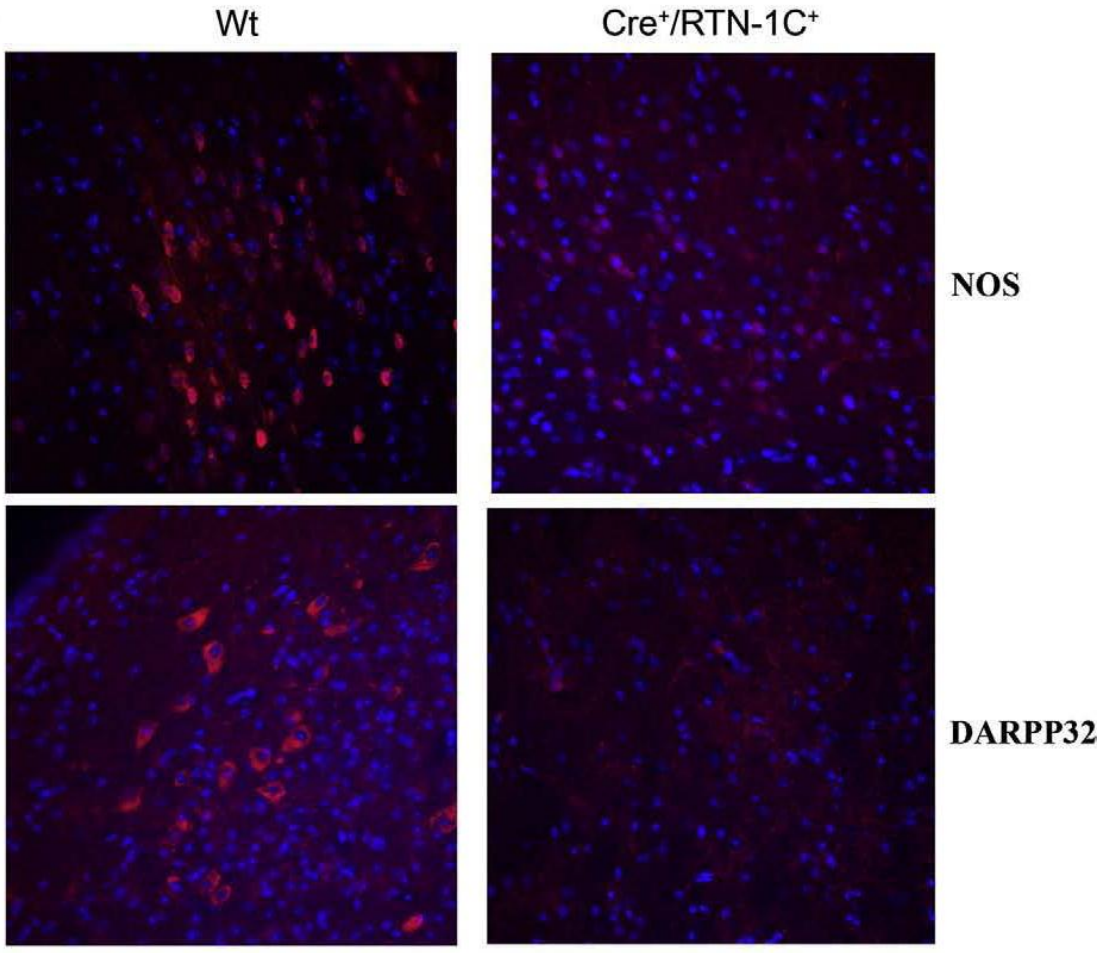

Fig. 5.10. Imaging analysis of RTN-1C-induced alteration of NOS and DARPP-32 genes experession in mouse brain.

Analysis of NOS and DARPP-32 expression by immunofluorescence in Wt and Cre+/RTN-1C+ brain sections taken from the cortex. The results shown are representative of three independent experiments. Images are taken at the same time of exposure. Magnification:20×. Brain sections were prepared by Dr.Marco Corazzari

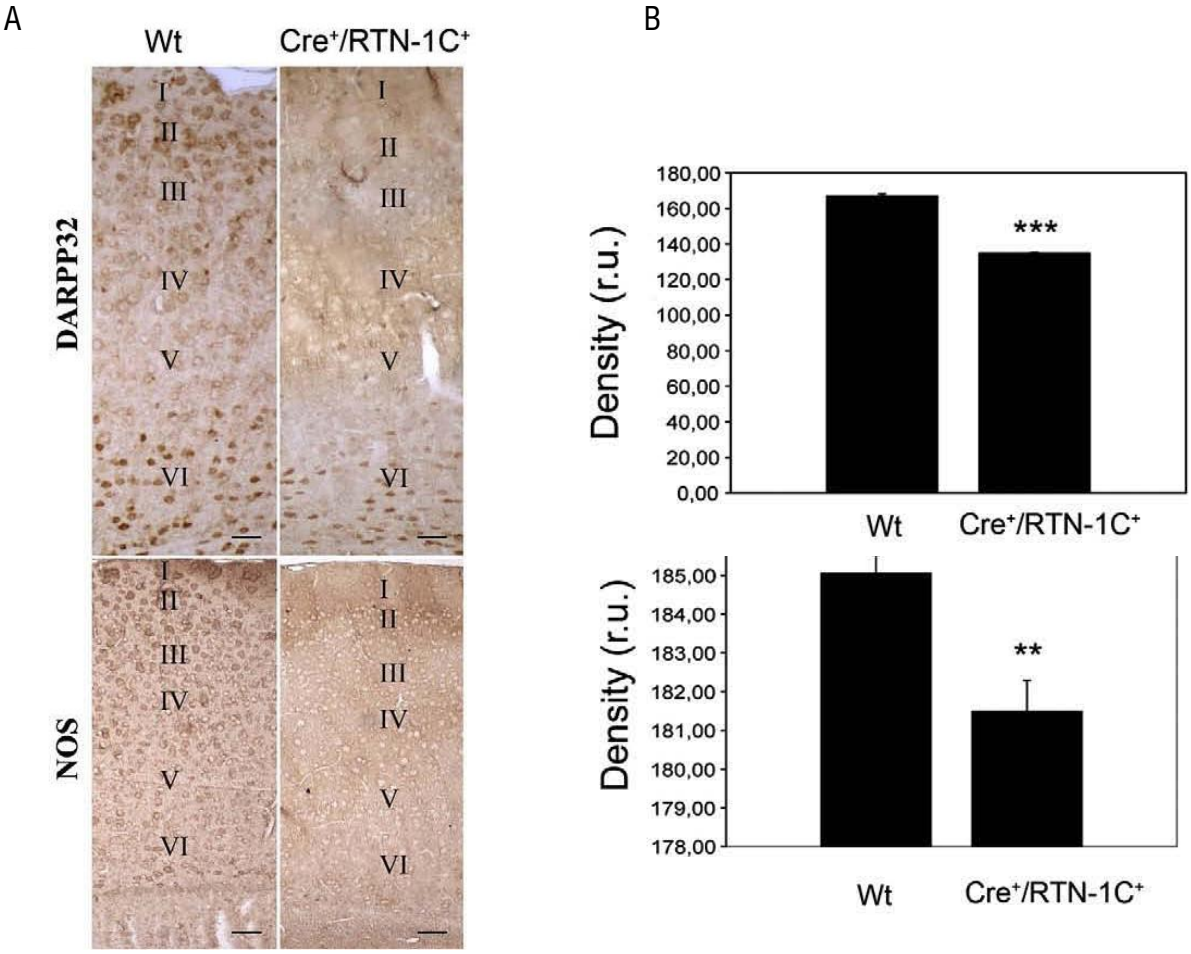

Fig. 5.11. Immuno-localization of DARPP-32 and NOS in RTN-1C transgenic mouse brain.

(A) Immunohistochemical localization of DARPP32 (upper panels) and NOS (lower panels) in Wt and the Cre+/RTN-1C+ mouse neocortex. I–VI, layers of the cerebral cortex. Bars, 100μm. (B) Densitometric analysis of immunostaining. **, $P < 0.01$. ***, $P < 0.001$. Immunohistochemistry and analysis were made by Dr.Marco Corazzari.

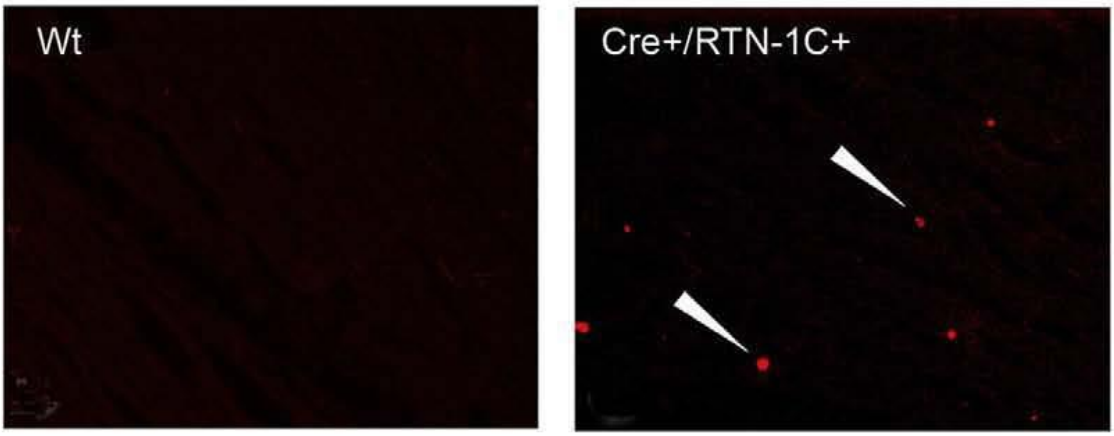

Fig. 5.12. TUNEL analysis of RTN-1C induced cell death in brain cortex. Photomicrographs of Wt and Cre+/RTN-1C+ brain sections stained with TUNEL. Arrowheads indicate the positive TUNEL staining of several cortical neurons in Cre+/RTN-1C+ transgenic mice.

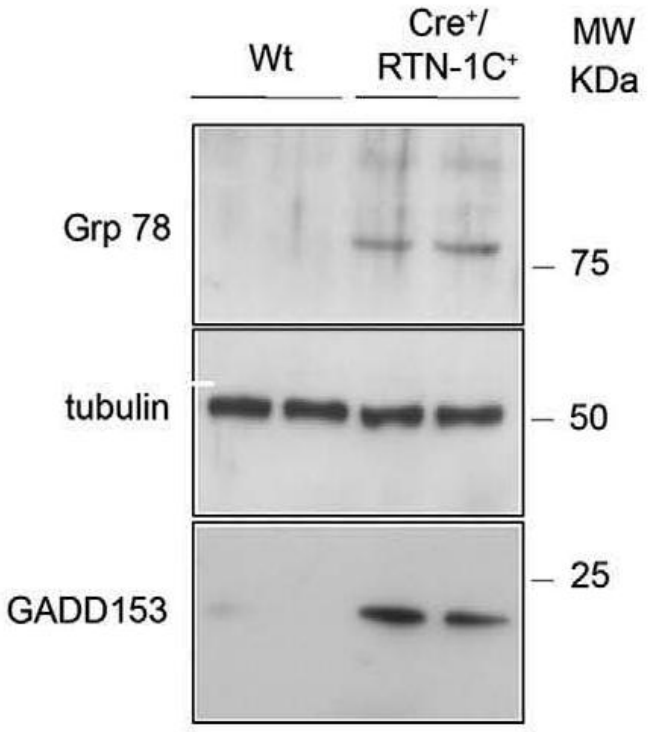

Fig. 5.13. Western blot analysis of RTN-1C induced ER stress markers in RTN-1C transgenic mice. Western blot analysis of UPR specific marker expression (Grp78 and GADD153) in cerebral cortex from two different Wt and Cre+/RTN-1C+ transgenic mice.

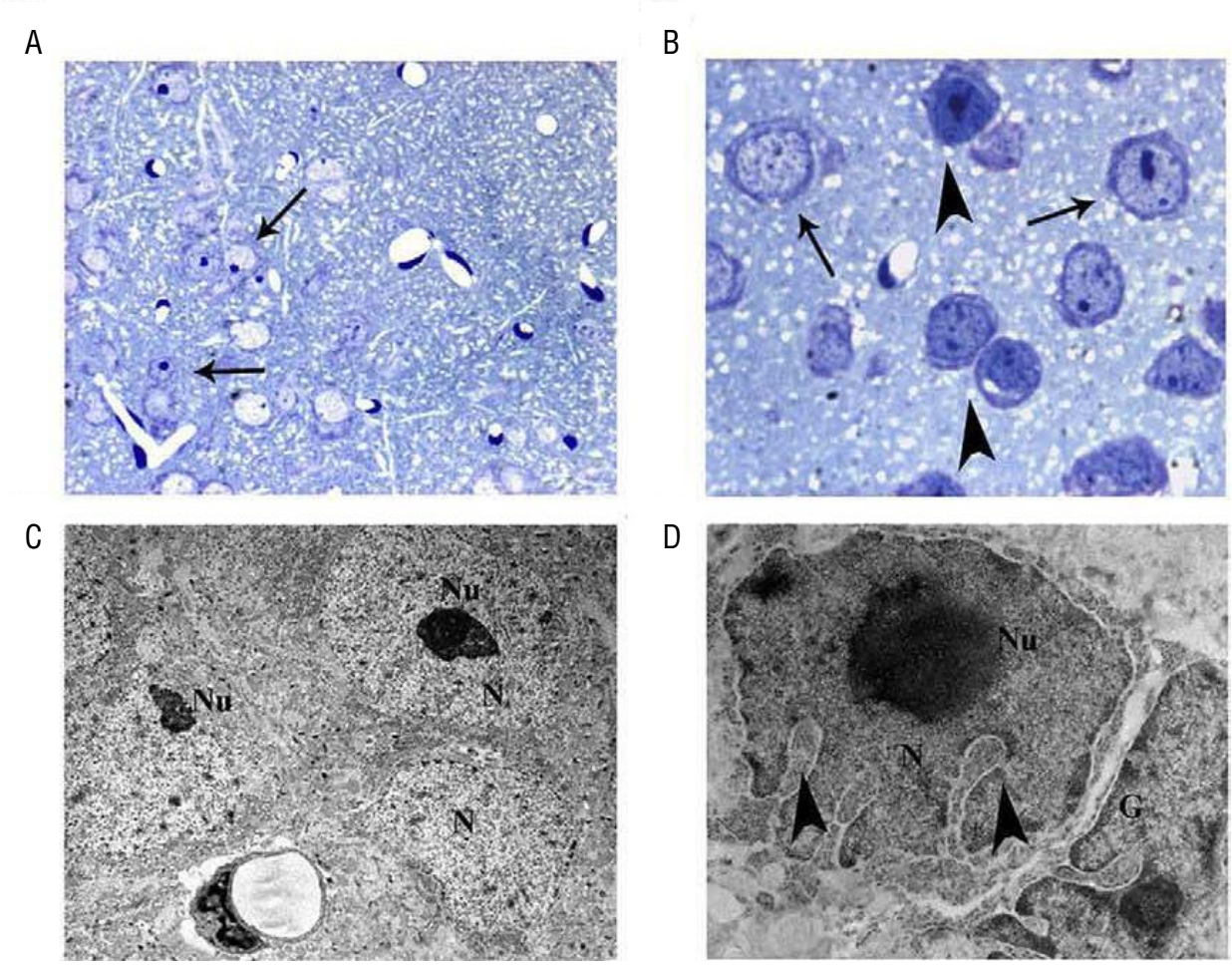

Fig. 5.14. Morphological analysis of RTN-1C induced cell death in brain cortex.

(A–D) Morphological analysis of brain cortex in Wt and Cre+/RTN-1C+ transgenic mice. Semi-thin section from Wt animals (A) shows neurons with normal morphology (arrows) while in the frontal cortex of Cre+/RTN-1C+ transgenic mice (B) some condensed neurons (arrowheads) are evident. In the lower panels the electron microscopy image of Wt mouse cortex (C) and with strongly altered morphology alteration is visible in a section of cortex from Cre+/RTN-1C+ transgenic mouse (D). The nuclear condensation is evident, the nuclear membrane shows numerous invaginations (arrowheads). N, nucleus; Nu, nucleolus. The image shows also a glial cell (G) displaying the same ultrastructural alterations. Data are representative of 30 images taken from 4 animals. Magnification A 40×, B 100×, C 4.400×, D 12.000×. Electron microscopy was done by Dr. Roberta Nardacci.